

# Task-Oriented Semantic Communication Systems Based on Extended Rate-Distortion Theory

Fangfang Liu, Wanjie Tong, Zhengfen Sun, and Caili Guo

**Abstract**—Considering the performance of intelligent task during signal exchange can help the communication system to automatically select those semantic parts which are helpful to perform the target task for compression and reconstruction, which can both greatly reduce the redundancy in signal and ensure the performance of the task. The traditional communication system based on rate-distortion theory treats all the information in the signal equally, but ignores their different importance to accomplish the task, which leads to waste of communication resources. In this paper, combined with the information bottleneck method, we present an extended rate-distortion theory which considers both concise representation and semantic distortion. Based on this theory, a task-oriented semantic image communication system is proposed. In order to verify that the proposed system can achieve performance improvement on different intelligent tasks, we apply the basic system trained with classification task to the system with object detection as the target task. The experimental results demonstrate that the proposed method outperforms the traditional and multi-task based communication system in terms of task performance at the same signal compression degree and noise interference degree. Furthermore, it is necessary to consider a compromise between rate-distortion theory and information bottleneck theory by comparing the pure rate-distortion scheme and the pure IB scheme.

**Index Terms**—Rate-distortion, information bottleneck, semantic communication, lossy image compression, intelligent tasks.

## I. INTRODUCTION

Semantic communication is categorized by Shannon and Weaver as a higher level beyond the traditional technical level of communication with a significant leap, where semantic defined as the meaning of source information is further exchanged over the symbols transmission in the technical level [1], [2]. As the tighter and deeper integration of communications and artificial intelligence, semantic communication is unfolding as a revolutionary paradigm of the next generation wireless networks [2], [3]. In this novel paradigm, not only the wireless transceivers are spanning from normal devices to intelligent entities with edge intelligence abilities, but also the applications are extended from connecting people to connecting intelligent unmanned systems with cloud intelligence abilities. For example, as the rapid development of intelligent connected vehicles and industrial internet, the intelligent entities like autonomous cars, robots, and machines are enabled by wireless communications and deep learning to collect, process, transmit, compute, and predict tremendous data with limited or even little human participation. Besides supporting human, the focus in semantic communication becomes mainly on supporting the intelligent entities to accomplish various intelligent tasks, especially the visual tasks like pedestrian monitoring, defect detecting, and security surveillance [4]. In these task-oriented semantic communication systems, one of the key challenges is **how to represent meaningful semantic information** at the transmitter to improve the performances of multiple visual tasks at the receiver.

Concise representation of source information is always an essential issue in order to reduce the transmission cost, which is especially limited by the finite frequency resources in wireless communications. For the text transmission, benefited from the powerful semantic extraction ability of the state-of-art natural language processing (NLP) techniques, there have been some investigations on end-to-end (E2E) communication semantic

communication systems [5]–[7]. While in the image case, how to effectively represent the semantic information in an image is still an open problem. In this paper, we mainly focus on the image case.

Rate-distortion theory plays an important role in lossy image compression for a long time, and image compression has been widely investigated in two categories in the traditional technical level of communication. One category is mainly based on the handcrafted time-frequency transforms such as JPEG and JPEG 2000 [8], [9], and the other is based on the flexible nonlinear transforms provided by deep learning, which is implemented mainly by auto-encoder [10]–[14]. These methods are committed to achieving a better trade off between the rate and the average reconstruction distortion of the compressed image. Here the reconstruction distortion in these methods is generally specified as the mean square error (MSE) between the original input image and the reconstructed image in pixels. Based on the rate distortion theory, the minimized reconstruction distortion in these methods can be expected given the rate constraint, which mainly aims to maintain the visual quality for human in limited wireless communication resources. However, reconstruction distortion causes communication systems to allocate a lot of bits on background pixels that are not helpful for subsequent intelligent tasks, resulting in a waste of resources.

Different from the general pixel-level reconstruction, literature [29] proposed reconstruction at the feature-level, thus taking a step toward semantic image transmission. However, feature reconstruction is still not enough, and this is essentially a further constraint on the quality of image itself. To sum up, whether the image is reconstructed on pixel-level or feature-level, image transmission itself does not directly consider the subsequent intelligent tasks.

Considering the performance of intelligent tasks directly, the Information bottleneck (IB) principle [15] aims to achieve the trade-off between concise representation and good predictive power on target task. Since it was proposed, there has been a lot of research on this theory. Recently, researchers have tried to use IB to explain deep neural networks [16], [17], and have made some interesting progress. Further, applying IB to image recognition could yield better performance than using other regular terms [18]. The essence of IB is to use task-specific distortion (hereinafter referred to as IB distortion) instead of task-independent reconstruction distortion. However, if only the distortion related to the task is considered, the original image will be greatly compressed and the output features will be specific to the target task, thus losing the generalization ability to perform other intelligent tasks. Inspired by this, we jointly optimize reconstruction distortion and IB distortion, and propose an semantic image communication system for intelligent task with good generalization ability among various intelligent tasks.

In brief, the main contributions of this paper are summarized as follows:

- Based on the traditional rate-distortion theory and information bottleneck principle, an extended rate-distortion theory is proposed, which aims to optimized the communication system for the purpose of trade-off between concise representation and semantic distortion, where the semantic distortion is referred to the proper trade-off

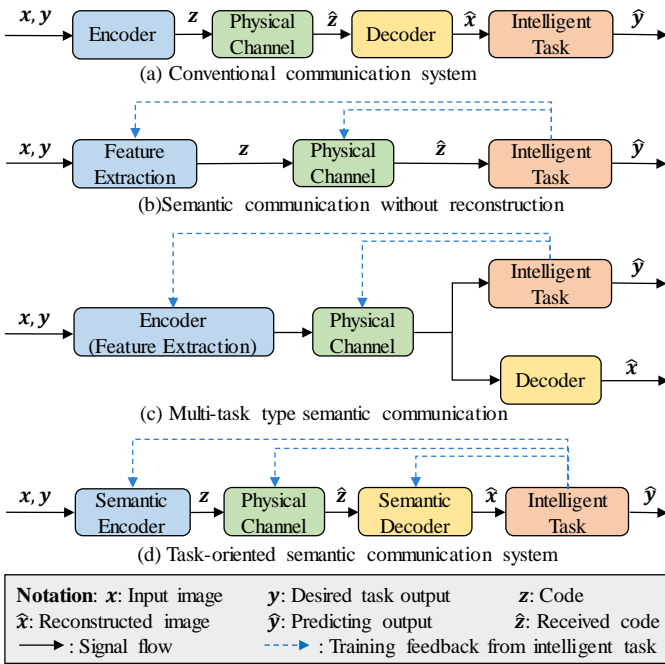


Fig. 1. Comparisons of different image communication frameworks with intelligent task: (a) conventional processing pipeline, (b) recently proposed semantic communication without reconstruction [24]–[26], (c) recently proposed multi-task type semantic communication with reconstruction [4], [27]–[31], and (d) our proposed semantic communication system with reconstruction. Note that the channel coding and decoding are ignored, which is not we focus on.

between reconstruction distortion and IB distortion.

- We build an task-oriented semantic image communication system based on the cascade of auto-encoder and intelligent task network. In order to make the reconstructed image perform the intelligent task better and have good generalization ability, we optimize the task-related IB distortion and reconstruction distortion simultaneously.
- In order to verify the generalization ability of the proposed system on different intelligent tasks, we transfer the semantic communication system trained on the classification task to the semantic communication system for object detection.
- Experimental results show that the proposed semantic image communication system is superior to the image communication system guided by reconstruction distortion or task distortion in terms of task’s performance at the same compression level. Besides, the system trained on the classification task can be directly applied to the object detection system, which still has a certain performance improvement.

The rest of this paper is organized as follows. Related works are reviewed in Section II. The system model is presented and a corresponding problem is formulated in Section III. Section IV shows the detailed description of the proposed semantic image communication system. The experimental results along with discussions are presented in Section V. Finally, conclusions are drawn in Section VI.

## II. RELATED WORK

### A. Definition and Measurement of Semantic Information

In the semantic information theory, the first critical problem is how to define and measure semantic information. Despite decades of development, this is still an open problem. There has been some exploratory research after Weaver proposed the three levels involved in communication [1]. Carnap et al. [19]

introduced the semantic information theory based on logical probabilities (as opposed to the statistical probabilities used in classical information theory) ranging over the contents. Barwise et al. [20] further proposed the principle of scene logic to define semantic information. Floridi et al. [21] introduced the theory of strongly semantic information. Though semantic information can be computed according to the logical-based definition, it is still challenging to implement the measurement because it is almost impossible to determine the standard logical probabilities of all the input random variables. On the other hand, for the images source, which is more complex, there are little theoretic research. The Information Bottleneck (IB) principle proposed by Naftali Tishby [15] provided a new idea to these problems by using mutual information to define and measure the meaningful or relevant information with an additional target variable, the author also claimed that mutual information provided a natural quantitative approach to the question of relevant information. Recently, with the great success of deep learning in extracting features from various signal resources, using DNNs to define and measure semantic information has become a new research direction [6], [22].

### B. Frameworks of Semantic Communication Systems

In this paper we mainly focus on the design of semantic communication system frameworks based on DNNs. With the effectiveness of DNNs in end-to-end physical layer communication systems [23], researchers have made some preliminary explorations in semantic communication systems.

For text transmission, Farsad et al. [5] proposed a joint source-channel coding implemented by a recurrent neural network (RNN), which is optimized for word error rate (WER). In order to further understand the sentence rather than independent words, Xie et al. [6] designed a deep semantic communication (DeepSC) system based on Transformer, and introduced the concept of sentence similarity. S Yao et al. [7] improved the Bi-directional Long Short-Term Memory (BiLSTM) and promoted the WER.

**Unlike texts, image’s semantics are more difficult to define due to its natural complexity, abstraction and objectivity. In general, the semantic information of images are considered as those information relevant to target tasks.** Among recent studies, there are two types of frameworks of semantic image communication system, non-reconstructed based and reconstructed based. The former considered the semantics as features highly relevant to specific task. In this framework type, as shown in Fig. 1(b), semantic communication system was usually designed for specific task. Lee et al. [24] designed a deep learning-constructed joint transmission-recognition scheme for the IoT devices by performing the feature extraction and recognition at the IoT device and server respectively. Along this line, Yang et al. [25] further compressed the transmitted data by introducing the semantic relationship between feature maps and semantic concept. Jankowski et al. [26] proposed a task-based compression scheme for input images for the person re-ID task, and pointed that in classification it is unnecessary to send feature maps to the receiver because the transmitter can execute the task locally and send only the predictive class label, in contrast, the transmitter can’t perform image retrieval alone due to missing gallery images.

**These non-constructed based semantic communication schemes often accompanied with specific task.** Once the task is determined, the semantic communication system’s application will be limited. **We aim to propose a more general framework.** Considering constructed based schemes, the basic scheme is shown in Fig. 1(a). Bourtsoulatz et al. [27] designed a joint source and channel coding image communication system based on convolutional neural networks (CNNs), where peak signal-to-noise ratio (PSNR) is used to measure the accuracy of image recovery at the receiver. By incorporating the channel

output feedback into the transmission system, Kurka et al. [28] improved the reconstruction quality at the receiver. In order to make reconstructed images similar to original images not only in pixel-level, but also in feature-level, based on the works of Yang et al. [29], Niu et al. [30] proposed a semantic communication system by jointly optimize the appearance loss and multi-scale discriminator loss. Though the reconstructed images are more similar with original images in both appearance and perception, the semantics relevant to task are still not considered. By incorporating the semantic information into the codec during image compression, Luo et al. [31] proposed a concept called deep semantic compression (DeepSIC) and designed two semantic compression networks by performing the semantic analysis after the feature extractor in the transmitter. In line with this idea, Patwa et al. [4] modified the auto-encoder networks and obtained better multi-task (classification and reconstruction) performance. The schemes proposed by [4], [31] are actually multi-task type semantic communication system, as shown in Fig. 1(c), where the multiple tasks will compete with each other for better performance. Motivated by this, we designed a task-oriented semantic communication system with cascaded structure, as shown in Fig. 1(d). **(The paper does not point out the difference in the feedback loop!!!)**

### C. Semantic Representation and Image Compression

**Semantic representation means using concise representation to express semantics.** The most relevant research about image's semantic representation is image compression. As a highly abstract and complex source, image contains abundant information. Traditional lossy compression methods, such as JPEG [8], JPEG2000 [9] and HEVC [32], rely on hand-crafted module design individually. Each module was designed with multiple modes and optimized for the rate-distortion to determine the best mode. Recently, a great number of learning-based image compression models utilizing auto-encoder architecture have been proposed, which have achieved great success with promising results [10]–[14]. Similar to traditional methods, these models were still optimized for rate-distortion, without considering the contents or semantics of images. Li et al. [33] proposed a content-weighted strategy to allocate more bits to the important parts of an image, which is determined by a simple fully connected network. Considering the region of interest (ROI) of an image, Cai et al. [34] designed an end-to-end optimized ROI image compression scheme, which achieved better visual quality and compression performance than traditional compression methods in ROI. Note that the contents of images are not semantics, and the compression scheme in [33], [34] didn't pay attention to the task performance. **In order to further realize the semantic compression, we consider the task feedback in our proposed method.**

### D. Rate Distortion and Information Bottleneck

Though some preliminary semantic communication systems have been proposed by researchers, to our best knowledge, there is no theoretical research in semantic information compression and extraction like rate-distortion theory in traditional lossy compression field. As an extension to rate-distortion theory, information bottleneck method was first proposed by Tishby et al. [15] in 1999. The author formulated a theoretic framework that finds concise representations for the source random variable that are as relevant as possible for a target random variable. And this method has proven to be useful for various supervised and unsupervised applications [35]–[37]. From a learning theoretic perspective, the mutual information between intermediate random variable and target random variable is a measure of performance, and the mutual information between source random variable and intermediate random variable is a regularization term [38]. Recently, IB has been used to explain

the optimization process of DNNs [16]. And the visual experiments in [17] show that the optimization process is indeed corresponding to the optimization objective of IB. Inspired by this, Alemi et al. [18] adopted a variational approximation to the IB, then optimized the supervised learning model constructed by DNN using the relaxed IB trade-off, and obtained better performance than other forms of regularization.

## III. SYSTEM MODEL AND PROBLEM FORMULATION

In this section, we formulate a semantic image communication framework giving consideration to both predicting precision and generalization capacity among multiple tasks.

### A. General framework

Consider such a communication scenario, in which the transmitter has collected some images and needs to send them to the receiver, and the received images will be used to complete various intelligent tasks in the receiver. Fig.2 shows the proposed semantic image transmission framework. In contrast to traditional image communication systems, here, both the transmitter and receiver are **AI agents**, and the goal of communication between them is no more than perceptual quality of images, but the ultimate performance in a variety of intelligent tasks. **Specifically**, the transmitter first collects the images, after semantic encoding and quantification, these codes will be sent to the receiver through the physical channel, and the receiver will get the decoded images after semantic decoding, then complete the subsequent intelligent tasks. **Since the core objective is to enable the reconstructed image to better complete the intelligent task, the ability of reconstructed image to complete the task should be considered in the process of image's encoding and decoding.**

**In this paper, we mainly focused on lossy image compression.** Let  $X$  denote random variable from the source image space\*. In general,  $X$  needs to be compressed to save bandwidth. The relevant variable  $Y$  is the desired output of intelligent task when corresponding  $X$  is feed to the task network. Semantic encoder maps the input to code space. Then the quantized code  $Z$  will be transmitted to the receiver through physical channel (**Channel coding is ignored for simplicity**). In the receiver, semantic decoder maps the noisy code to reconstructed image  $\hat{X}$ . At last, intelligent task network takes  $\hat{X}$  as input and outputs the predict result  $\hat{Y}$ . **For ease of exposition we assume here that all of these sets  $X, Y, Z$  and  $\hat{X}$  are finite, that is, a continuous space should first be quantized. This is consistent with the fact that we are only access to finite data  $X$  and  $Y$ , and the compressed codes  $Z$  should to be quantized, resulting the finite  $\hat{X}$ .**

As the classic lossy compression theory, rate distortion theory characterizes the trade-off between rate and distortion by the rate distortion function  $R(D)$  or distortion rate function  $D(R)$ . Here rate  $R$  is  $I(X; Z)$ , **which is the minimal number of bits per symbol so that the source (input signal) can be approximately reconstructed at the receiver (output signal) without exceeding an expected distortion.** Distortion  $D_{RD}$  is usually assessed by mean squared error (MSE) between  $X$  and  $\hat{X}$ , or other metrics for high quality of appearance.

The information bottleneck (IB) method extends the rate-distortion theory by replacing the distortion function with the **relevant information distortion**. Specifically, IB proposed the concept of relevant information and pointed out that in lossy image compression, the selection of distortion function actually corresponds to the selection of relevant features [15]. IB principle characterizes the trade-off between rate and relevant information distortion. The definition of rate is consistent

\*In this work,  $X, Y, Z, \hat{X}$  are random variables,  $x, y, z, \hat{x}$  and  $\mathbf{x}, \mathbf{y}, \mathbf{z}, \hat{\mathbf{x}}$  are instances of corresponding random variables.

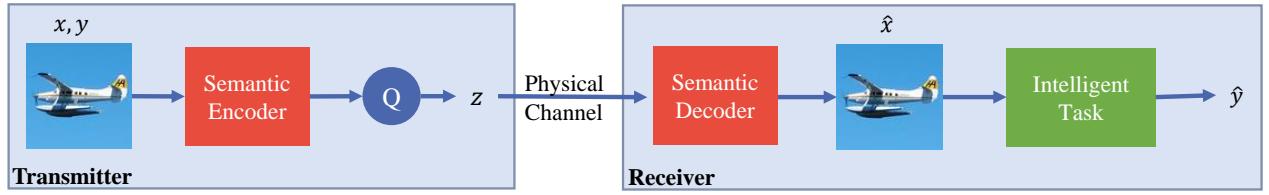


Fig. 2. Proposed semantic image communication framework

with the rate-distortion theory, while distortion is different. According to IB method, relevant information distortion refers to the amount of information that  $\hat{X}$  loses about  $Y$  compared to  $X$ . Denote  $D_{IB}$  as the distortion function in IB.

In the image communication system, if we use the traditional rate distortion performance as our optimized object, the images will be reconstructed for the purpose of keeping as high perceptual quality as possible, without considering the performance of subsequent tasks, which means the whole system try its best to retain all the information of the original image. **Any deterioration in image quality during communication can have a significant impact on the reconstructed image's ability to perform subsequent intelligent tasks [50].** On the other hand, if only a single intelligent task at the receiver is considered, that is, only the information relevant to this task is **retained/protected**, just like the practice of information bottleneck, although the task can be better completed under the condition of **great compression**, this will inevitably lose a lot of structure information of the original image, resulting in the reconstructed image can not well complete other intelligent tasks, that is, generalization performance is deteriorated. Motivated by this intuition, we propose a semantic image transmission framework, considering both predictive performance and generalization capability among different tasks. Predictive performance requires more task-relevant information to be retained, and generalization capability ensure that the structure information of original image is not destroyed seriously. Therefore, we call our method information theoretic trade-off.

### B. Semantic Distortion Measurement

We will give the proposed semantic distortion measurement based on the trade-off of rate distortion theory and information bottleneck principle.

In order to ensure that the reconstructed images can better complete the task, we should minimize the relevant information distortion  $D_{IB}(X, \hat{X})$

$$D_{IB}(X, \hat{X}) = I(X; Y) - I(\hat{X}; Y) \quad (1)$$

In the standard information bottleneck method, the relevant information distortion function between  $x$  and  $\hat{x}$  is represented by  $D_{KL}[p(y|x)|p(y|\hat{x})]$  [15], and the expectation of relevant information distortion is  $I(X; Y|\hat{X})$  [16]. We can prove that these definitions are equivalent under certain conditions, and the definition of equation 1 is used here because this expression more intuitively illustrates the reduction of relevant information. See Appendix A for detailed proof.

**In order to ensure generalization among different intelligent tasks**, we should minimize  $D_{RD}(X, \hat{X})$ ,

$$D_{RD}(X, \hat{X}) = \sum_x \sum_{\hat{x}} p(x, \hat{x}) d_{RD}(x, \hat{x}) \quad (2)$$

here we use the MSE as appearance distortion function,

$$d_{RD}(x, \hat{x}) = (x - \hat{x})^2 \quad (3)$$

Considering the trade-off between two distortion measures, we can define the following semantic distortion measure,

$$D_S(X, \hat{X}) = D_{RD}(X, \hat{X}) + \beta D_{IB}(X, \hat{X}) \quad (4)$$

where  $\beta$  controls the trade-off between predicting precision and generalization capacity.

### C. Problem Formulation and Solution

If minimizing semantic distortion  $D_S$  is our only optimized objective, the best solution would be an identity map of original data ( $Z = X$ ), but for communication systems, it is obviously very wasteful to transmit raw data directly without compression. Similar to rate distortion optimization, we apply a constraint on the rate  $I(X; \hat{X})$ , which is given by

$$I(X; \hat{X}) = \sum_x \sum_{\hat{x}} p(x, \hat{x}) \log \left[ \frac{p(x, \hat{x})}{p(x)p(\hat{x})} \right] \quad (5)$$

and the constraint on  $I(X, \hat{X})$  is

$$I(X, \hat{X}) \leq I_C \quad (6)$$

then we can get the following optimization problem,

$$\min_{p(\hat{x}|x): I(X, \hat{X}) \leq I_C} D_S(X, \hat{X}) \quad (7)$$

Combined with equation (4), let's also consider the normalization of conditional probability  $p(\hat{x}|x)$ , optimization problem (7) can be converted to

$$\min_{\substack{p(\hat{x}|x): I(X, \hat{X}) \leq I_C \\ \sum_{\hat{x}} p(\hat{x}|x) = 1}} D_{RD}(X, \hat{X}) + \beta D_{IB}(X, \hat{X}) \quad (8)$$

According to equation (1), since  $I(X; Y)$  is a constant with respect to dataset, optimization problem (8) can be converted to,

$$\min_{\substack{p(\hat{x}|x): I(X, \hat{X}) \leq I_C \\ \sum_{\hat{x}} p(\hat{x}|x) = 1}} D_{RD}(X, \hat{X}) - \beta I(\hat{X}; Y) \quad (9)$$

This optimization problem can be solved by the Lagrange multiplier method, and the only variable is  $p(\hat{x}|x)$ . The complete process for solving this problem is shown in Appendix B. Here we directly give the formal solution.

$$\begin{cases} p_k(\hat{x}|x) = \frac{p_k(\hat{x}) e^{-\lambda^{-1} d_S(x, \hat{x})}}{\sum_{\hat{x}} p_k(\hat{x}) e^{-\lambda^{-1} d_S(x, \hat{x})}} \\ p_{k+1}(\hat{x}) = \sum_x p(x) p_k(\hat{x}|x) \\ p_{k+1}(y|\hat{x}) = \sum_y p(y|x) \frac{p_k(\hat{x}|x) p(x)}{p_k(\hat{x})} \end{cases} \quad (10)$$

By iteratively solving the above self-consistent equations, we can obtain the optimal trade-off between rate and semantic distortion.

**The above process assumes that the probability distribution of the data is available and the distribution is discrete.** Although this process can be extended to the case of

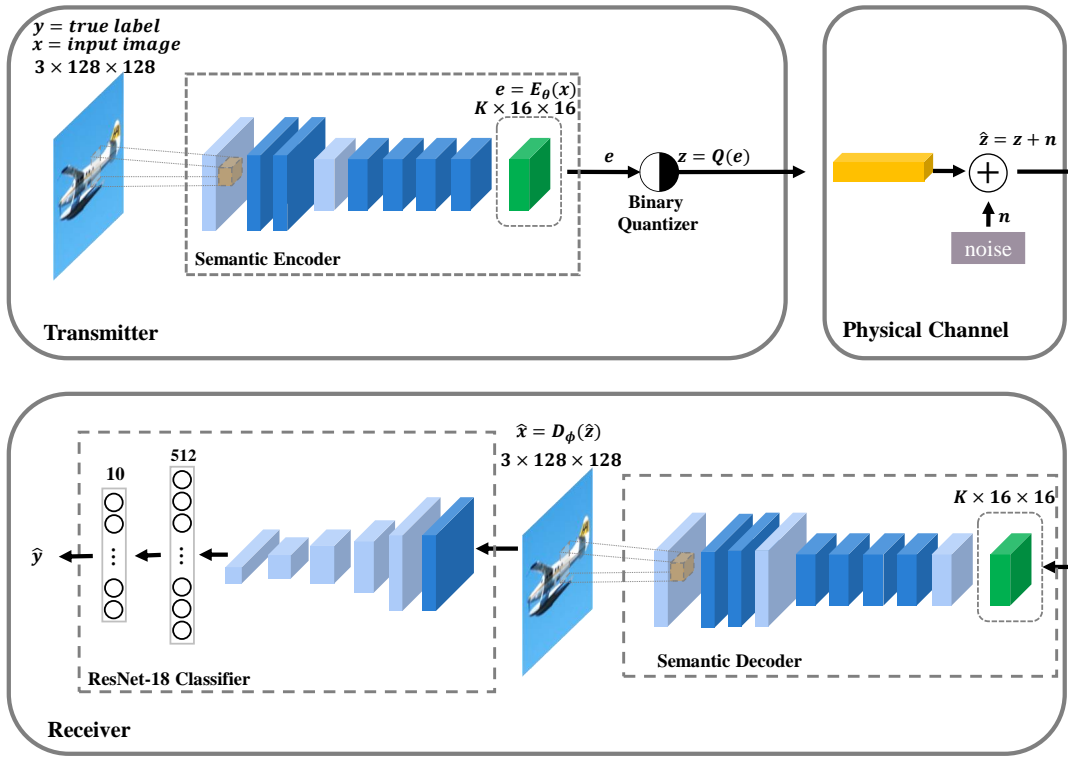


Fig. 3. The architecture of proposed semantic image transmission system

continuous variables, it is often difficult to calculate the probability distribution for high-dimensional data such as images. Therefore, it is difficult to use the iterative algorithm. Observing the optimization problems (9), the essence of which is find the smallest semantic distortion of conditional probability  $p(\hat{x}|x)$  under the condition of certain compression. If the optimization objective can be written as an expression and the gradient can be calculated by back propagation, then the conditional probability can be solved by using a **deep neural network**. In the next section we will build a detailed semantic image transmission system based on **DNNs**.

#### IV. PROPOSED SEMANTIC IMAGE COMMUNICATION SYSTEM

Based on the theoretical analysis of the previous section, this section will design and implement a concrete semantic image communication system. **First, we introduce the components of proposed system architecture in detail. Then, the practical loss function is given by relaxing the mutual information optimization object for ease of computation during the training process. Meanwhile, we point out that the loss function has close relationships with mutual information. Next, transfer validation is adopted to make the proposed system applicable to different intelligent tasks. Finally, corresponding training algorithms are presented.**

##### A. System Architecture

The proposed system is shown in the Fig. 3. The overall architecture consists of three parts, i.e. transmitter, channel and receiver. Transmitter is composed of semantic encoder and binary quantifier. The general AWGN channel is adopted here. Receiver is mainly composed of semantic decoder and ResNet-18 classifier. It is important to note that we adopt the classification task as our basic intelligent task. The whole architecture

is an end-to-end deep neural network. Since the subsequent intelligent task of the receiver will have a positive impact on the performance of the whole network, the images reconstructed by the receiver contain more task-relevant information and have a certain generalization ability among different intelligent tasks. Compared with the general auto-encoder, we call it semantic auto-encoder here. The implementation details of each part are described below.

1) *Semantic Encoder and Decoder*: As shown in Fig. 3, the semantic encoder and decoder used in our system are fully convolutional networks. Following [33], the encoder network consists of three convolution layers and three residual blocks. Except for the last convolution layer, which is followed by a sigmoid activation function so that encoder's output can be in range of  $[0, 1]$ , previous convolution layers and residual blocks are followed by relu activation function. Each residual block has two convolution layers. The whole encoder achieves eight times subsampling on the spatial dimension of the image. Specifically, the input image  $x$  is first convolved with 128 filters with size  $8 \times 8$  and stride 4 and followed by one residual block. The feature maps are then convolved with 256 filters with  $4 \times 4$  and stride 2 and followed by two residual blocks. Finally, feature maps are convolved with  $N$  filters with  $3 \times 3$  and stride 1 to yield semantic encoder output  $E(*)$ . It should be noted that we set different  $K$  for different levels of compression.

The network of decoder  $D(*)$  is almost symmetric to that of the encoder except some difference in the numbers of convolutional layers and filters in each layer. In addition, we apply depth-to-space method to implement upsampling.

**At last, it should be noted that we call it a semantic encoder because the ultimate goal of encoding is no longer to accurately recover an image or simply to complete a task, but to consider a trade-off between prediction precision and generalization ability among various intelligent tasks.**

2) *Binary Quantizer*: Quantization is necessary for a digital communication system, especially for the lossy compression



communication system, because continuous variables need infinite numbers of bits to represent, which is impossible to realize. In the whole end-to-end semantic image communication network, quantization is the only non-differentiable component. The derivative of the rounding function is zero everywhere, rendering gradient descent ineffective. In order to initiate the training process, this problem should be solved. Some smooth approximations are proposed in related works. Balle et al. [10] implemented the quantization by an additive uniform noise as  $z_{kij} = e_{kij} + u$ .<sup>†</sup> As rounding operation is like adding an uniform noise on the signals. Thesis et al. [11] proposed a proxy differentiable function to replace the non-differentiable rounding in the back propagation. The form of the proxy function is simple, which is  $z_{kij} = e_{kij}$ . So  $\frac{dz_{kij}}{de_{kij}} = 1$ . Toderici et al. [12] used a stochastic binarization function as  $z_{kij} = -1$  when  $e_{kij} < 0$ , and  $z_{kij} = 1$  otherwise. **Here we point out that either using a proxy function, or adding an uniform noise, their derivatives of corresponding rounding functions are both 1 in the back propagation.**

In our system, the binary quantization is implemented by using a simple proxy function. Because the semantic encoder's last convolution layer is activated by sigmoid function, the values of  $e = E(x)$ 's should be in range of  $[0, 1]$ . In the forward paopagation, the binarizer is defined as

$$z_{kij} = \begin{cases} 1, & \text{if } e_{kij} > 0.5, \\ 0, & \text{if } e_{kij} \leq 0.5. \end{cases} \quad (11)$$

In the back propagation, the proxy function of binarizer is defined as

$$\tilde{z}_{kij} = \begin{cases} 1, & \text{if } e_{kij} > 1, \\ e_{kij}, & \text{if } 0 \leq e_{kij} \leq 1, \\ 0, & \text{if } e_{kij} < 0. \end{cases} \quad (12)$$

So the derivatives of the proxy function is,

$$\frac{d\tilde{z}_{kij}}{de_{kij}} = \begin{cases} 1, & \text{if } 0 \leq e_{kij} \leq 1, \\ 0, & \text{otherwise.} \end{cases} \quad (13)$$

After quantization, we can compute the bit per pixel (bpp) as following,

$$bpp = \frac{K \times 16 \times 16}{128 \times 128} = \frac{K}{64}. \quad (14)$$

Once again, for ease of explanations, we didn't take the entropy coding into account, so the bpp here we obtain is actually the upper bound of bpp for different compression level, which can be further compressed by entropy encoding. In the later of this paper, Without ambiguity, we will refer the upper bound bpp as bpp.

3) *Physical channel*: [3] Noise is caused by the physical channel impairment, such as, additive white Gaussian noise (AWGN), fading channel, and multiple path, which incurs the signal attenuation and distortion. In order to realize E2E training of the encoder and the decoder, the channel must allow back-propagation, so that it can be incorporated into the overall framework.

In this paper, we mainly consider the AWGN channel for simplicity while focus on the performance of semantic coding and decoding. To be specific, there is a independent gaussian source, which produce noise  $n \sim \mathcal{N}(0, \sigma^2 I_d)$ , where  $\sigma^2$  is the average noise power, and  $d$  is the total dimensions of  $z$ . So we attain the noisy output  $\hat{z} = z + n$ . It is obviously that  $\frac{d\tilde{z}_{kij}}{dz_{kij}} = 1$ .

4) *Classifier*: As a basic intelligent task in the receiver, classifier plays a critical role in the semantic image communication system. If we remove classifier, this system will degrade to a normal auto-encoder for image transmission,

which is optimized for the rate-distortion performance. Once adding a intelligent task, which means introducing a task-relevant information distortion, our auto-encoder is no longer a unsupervised network, the optimized objective will change from previous rate-distortion trade-off  $L = R + \lambda D$  to rate-semantic distortion trade-off  $L_S = R + \lambda D_S$ . As shown in Fig. 3, the classic ResNet-18 network followed by a fully connected layer is used as our classifier.

Above we have introduced the specific implementation of each part in the system, here we will put them together and track the data flow along the system architecture. When the transmitter need to send an image  $x$  with the desired output  $y$  (the desired output is the true label in classification task) to the receiver, the convolutional semantic encoder maps the image to code space and outputs  $e = E(x)$ . Then the binary quantizer takes round operation on  $e$  and yields  $z = Q(e)$ . **For ease of exposition we don't consider the entropy coding, which doesn't introduce any distortion.** The compression level is decided by the channel numbers of encoder' output. Then the codes  $z$  pass through the physical channel, yielding noisy codes  $\hat{z} = z + n$ . Next, the convolutional semantic decoder decodes  $\hat{z}$  and outputs reconstructed image  $\hat{x} = D(\hat{z})$ . Finally,  $\hat{x}$  is fed into the classifier, which outputs the predicted result  $\hat{y}$ . **Due to the effectiveness introduced by the classifier network, compared with traditional image communication systems, our reconstructed images will contain more semantic information.**

## B. Loss Function and Mutual information

1) *Loss Function*: The goal of the system is to minimize the semantic distortion while reducing the rate of symbols to be transmitted, which implies the following loss function,

$$\mathcal{L} = R + \lambda D_S(X, \hat{X}) \quad (15)$$

since the compression level is controled by the number of output  $z$ ' channels, this optimized objective will be simplified by fixing the rate  $R$ ,

$$\mathcal{L}_R = D_S(X, \hat{X}) \quad (16)$$

where

$$D_S(X, \hat{X}) = D_{RD}(X, \hat{X}) + \beta D_{IB}(X, \hat{X}) \quad (17)$$

$D_{RD}(X, \hat{X})$  is a fixed distortion function w.r.t.  $X$  and  $\hat{X}$ , so it can be computed once we obtain the input images  $X$  and reconstructed images  $\hat{X}$ . Computing  $D_{IB}(X, \hat{X})$  is challenging, according to equation (1)  $I(X; Y)$  can be regard as a constant, but  $I(\hat{X}; Y)$  is hard to compute. So minimizing  $D_{IB}(X, \hat{X})$  is equal to maximizing  $I(\hat{X}; Y)$ .

Next, we derive a variational upper bound of  $D_{IB}(X, \hat{X})$  by approximating a variational lower bound of  $I(\hat{X}; Y)$ .

According to the definition of mutual information

$$I(\hat{X}; Y) = H(p(Y)) - H(p(Y|\hat{X})) \quad (18)$$

where  $p(Y)$  and  $p(Y|\hat{X})$  are the distributions of  $Y$  and recognition model respectively. Consider a variational approximation  $q(Y|\hat{X})$ . The non-negativity of KL divergence leads to the following variational lower bound,

$$\begin{aligned} I(\hat{X}; Y) &= H(p(Y)) - H(p(Y|\hat{X})) \\ &\geq H(p(Y)) - H(p(Y|\hat{X})) \\ &\quad - D_{KL}(p(Y|\hat{X}) || q(Y|\hat{X})) \\ &= H(p(Y)) + \mathbb{E}_{p(Y, \hat{X})} [\log q(Y|\hat{X})] \end{aligned} \quad (19)$$

in the last line we've used the following identity,

$$\begin{aligned} -\mathbb{E}_{p(Y, \hat{X})} [\log q(Y|\hat{X})] &= D_{KL}(p(Y|\hat{X}) || q(Y|\hat{X})) \\ &\quad + H(p(Y|\hat{X})) \end{aligned} \quad (20)$$

<sup>†</sup>  $e_{kij}$  and  $z_{kij}$  denote the elements in  $e$  and  $z$ , k,i,j represent the corresponding channel and spatial index, respectively

so we get the following variational upper bound,

$$\begin{aligned} D_{IB}(X, \hat{X}) &= I(X; Y) - I(\hat{X}; Y) \\ &\leq I(X; Y) - H(p(Y)) \\ &\quad - \mathbb{E}_{p(Y, \hat{X})} [\log q(Y|\hat{X})] \end{aligned} \quad (21)$$

Notice that  $I(X; Y) - I(\hat{X}; Y)$  is a constant, which is independent of our optimization procedure and so can be ignored.

Above all, we know that,

$$\min D_{RD}(X, \hat{X}) + \beta D_{IB}(X, \hat{X}) \quad (22)$$

can be relaxed to minimizing its upper bound,

$$\min D_{RD}(X, \hat{X}) + \beta \mathbb{E}_{p(Y, \hat{X})} [\log q(Y|\hat{X})] \quad (23)$$

Here we adopt the mean square error function as our  $D_{RD}$ ,

$$D_{RD}(X, \hat{X}) = MSE(X; \hat{X}) = \sum_x \sum_{\hat{x}} \|x - \hat{x}\|^2 \quad (24)$$

In addition, we point out that the negative expectation term  $-\mathbb{E}_{p(Y, \hat{X})} [\log q(Y|\hat{X})]$  is actually the usual **cross-entropy loss**  $CE(Y, \hat{Y})$  in supervised learning.

Put everything together to get the following objective function which we try to minimize:

$$\mathcal{L}_R = MSE(X, \hat{X}) + \beta CE(Y, \hat{Y}) \quad (25)$$

**With this loss function, we can conduct our training experiment easily. But before this, we will further analysis this loss function from information theoretic by establishing relationship with mutual information.**

2) *Mutual Information*: Mutual information (MI) is a fundamental quantity for measuring the relationship between random variables. Minimizing or maximizing MI has gained considerable interests in a wide range of deep learning tasks. Similar to the idea in [16], which suggests using MI as the measurement of the quality of DNN. In our proposed semantic image communication system, MI also plays an important role in the following two aspects.

First, as a semantic image communication system, semantic information measurement is necessary. We consider the information relevant to various target tasks as semantic information, which should be saved as much as possible. MI provides a natural quantitative approach to relevant information. By encouraging the system capture as much as meaningful information and discard as much as information irrelevant to any target tasks, we can realize a semantic image communication system from the information theoretic view point.

Second, the optimization objective applied in our system, i.e. (15), actually has close relationship with MI. And the practical loss function adopted in the experiment, i.e.(25), is a relaxed version of (15). As shown in (15) and (17), the optimization objective consists of rate  $R$ , traditional distortion  $D_{RD}$  and single task relevant distortion  $D_{IB}$ . Next we will prove that all of the three parts have close connection with MI.

Rate  $R = I(X; \hat{X})$ , which is the MI between  $X$  and  $\hat{X}$ . On the one hand, this MI determine the minimal number of bits per pixel, and this is a theoretical lower bound. On the other hand, it also indicates the information about input  $X$  contained in the code  $\hat{X}$ . In general, the more this information is, the better reconstruction quality will be achieved. According to the data processing inequality,

$$I(X; \hat{X}) \leq I(X; Z) \quad (26)$$

$D_{RD}$  is the MSE between input  $X$  and reconstruction output  $\hat{X}$ , as shown in equation (24). MSE is the direct measurement of the difference between two variables, while the MI quantify the similarity between two variables. These two metrics appear to be moving in opposite directions. In practice,  $MSE(X; \hat{X})$  is indeed related to  $I(X; Z)$ .

According to the definition of MI,

$$I(X; Z) = H(X) - H(X|Z) \quad (27)$$

Because  $H(X)$  is a constant when dataset  $X$  is selected, we mainly focus on  $H(X|Z)$ .

$$\begin{aligned} H(X|Z) &= - \sum_x p(x) \sum_z p(z|x) \ln(p(x|z)) \\ &= \mathbb{E}_{x \sim p(x)} [\mathbb{E}_{z \sim p(z|x)} [-\ln(p(x|z))]] \end{aligned} \quad (28)$$

where  $p(x|z)$  is the semantic decoder, if we assume it follows the multivariate gaussian distribution with a fixed diagonal covariance  $\sigma^2$ ,

$$p(x|z) = \mathcal{N}(x; \mu, \sigma^2 I_D) \quad (29)$$

where  $\mu = D_\phi(z) = \hat{x}$ .  $D$  is the total dimension of  $x$ . So

$$p(x|z) = \frac{1}{\prod_{i=1}^D \sqrt{2\pi\sigma_i^2}} \exp\left(-\frac{1}{2} \left\| \frac{x - \hat{x}}{\sigma^2} \right\|^2\right) \quad (30)$$

then,

$$-\ln(p(x|z)) = \frac{1}{2} \left\| \frac{x - \hat{x}}{\sigma^2} \right\|^2 + \frac{D}{2} \ln 2\pi + \frac{1}{2} \sum_{i=1}^D \ln \sigma_i^2 \quad (31)$$

where the first term is the scaled MSE. Combine the equations (27), (28) and (31), we can find that if we use MSE as the loss function, minimizing  $MSE(X; \hat{X})$  means maximizing  $I(X; Z)$ . **This is intuitive and reasonable that the more information about  $X$  is contained in  $Z$ , the better construction quality of  $\hat{X}$  is.**

Single task relevant distortion  $D_{IB}$  is defined by the reduction of MI, as shown in (1). Minimizing  $D_{IB}$  means maximizing  $I(\hat{X}; Y)$ . According to the data processing inequality,

$$I(\hat{X}; Y) \geq I(\hat{Y}; Y) \quad (32)$$

Above all,  $Z$  and  $\hat{Y}$  are two critical variables in the whole end-to-end communication link. Meanwhile,  $Z$  and  $\hat{Y}$  are bottleneck variables (which have the minimal number of dimension) of semantic codec and classifier respectively. **So computing MI about these two variables is necessary.**

**Despite being a critical quantity across a wide range of domains, mutual information has historically been difficult to compute. The exact calculation requires closed forms of density functions and a tractable log-density ratio between the joint and marginal distributions. In most machine learning tasks, only samples from the joint distribution are accessible. Therefore, sample-based MI estimation methods have been proposed.**

[39] introduces a Mutual Information Neural Estimator (MINE), which treats MI as the Kullback-Leibler (KL) divergence between the joint and marginal distributions, and converts it into the dual representation:

$$I_{\text{MINE}} := \mathbb{E}_{p(x,y)} [T_\theta(x,y)] - \log \left( \mathbb{E}_{p(x)p(y)} \left[ e^{T_\theta(x,y)} \right] \right), \quad (33)$$

where  $T_\theta(x,y)$  is the function parametrized by a neural network, which takes samples  $x, y$  as input. Along with this method, the estimation of mutual information between high dimensional continuous random variables can be achieved by gradient descent over neural networks.

Recently, [40] introduce a Contrastive Log-ratio Upper Bound (CLUB). Specifically, CLUB bridges mutual information estimation with contrastive learning where MI is estimated by the difference of conditional probabilities between positive

and negative sample pairs, which is

$$I_{\text{CLUB}} := \mathbb{E}_{p(x,y)} [\log p(y|x)] - \mathbb{E}_{p(x)} \mathbb{E}_{p(y)} [\log p(y|x)]. \quad (34)$$

where  $p(y|x)$  is the conditional distribution of  $y$  given  $x$ . When  $p(y|x)$  is not provided, we can use a variational distribution  $q(y|x)$  to approximate  $p(y|x)$ , and  $q(y|x)$  is usually implemented by the neural network.

MINE estimates the MI through the lower bound. CLUB estimates the MI through the upper bound. In our application, it doesn't matter whether the bounds are upper or lower. We are more concerned about the accuracy of the estimate. According to the comparison experiments in [40], CLUB achieves the best accuracy.

### C. Transfer Performance for Different Tasks

A very important motivation to reconstruct images semantically is to ensure the transfer performance of the model between different tasks. For the multi-task learning model used in [4], if the receiver need to perform a different task, the network structure should to redesigned carefully. In contrast, our method is highly flexible in transferring to other tasks, and the only thing to do is replace the classification network with the mature target network.

In reality, the receiver usually need to perform various tasks when facing different scenes. The proposed semantic image communication system tries improve the performance of all intelligent tasks as possible, not just a single target task like the case in IB method. As an example, we take object detection as our another target task to verify the generalization performance of SICS. Specifically, we replaced the classification network in the receiver with a mature object detection network, which is RFBNet [41]. And the semantic auto-encoder trained by classification task remained unchanged. If semantic auto-encoder can reconstruct images with more semantic information, this transfer performance should be improved.

### D. Algorithms

#### Algorithm 1 Semantic image transmission training algorithm

**Input:** The background knowledge  $\mathcal{K}$ , i.e. dataset.

- 1: Train a classifier  $F_X$  with input dataset  $\mathcal{K}$ ;
- 2: Train a auto-encoder  $E_\theta$  and  $D_\phi$  with input dataset  $\mathcal{K}$ ;
- 3: Put the classifier behind the auto-encoder, like Fig.3. Load all pretrained network's parameters and freeze the parameters of  $F_X$ ;
- 4: **while** Stop criterion is not met **do**
- 5:   **Forward:**  $X \rightarrow \hat{X} = D_\phi(E_\theta(X))$
- 6:    $\hat{X} \rightarrow \hat{Y} = F_X(\hat{X})$ ;
- 7:   **Loss:**  $\mathcal{L}_R = \text{MSE}(X, \hat{X}) + \beta \text{CE}(Y, \hat{Y})$
- 8:   **Back-propagation:**  $\mathcal{L}_R \rightarrow \frac{\partial \mathcal{L}_R}{\partial W_{cae}}$ ;
- 9:   **Update parameters:**  $W_{cae} := W_{cae} - lr \frac{\partial \mathcal{L}_R}{\partial W_{cae}}$
- 10: **end while**

**Output:** The parameterized networks  $E_\theta^*$  and  $D_\phi^*$ .

Algorithm 1 describes the training process of the proposed method. In the preparation stage, a classifier and an convolutional auto-encoder need to be trained separately, and then these two networks are incorporated into our communication system for joint fine-tuning training, as shown in Fig.1.

Algorithm 2 and algorithm 3 are subalgorithms of algorithm 1, and they describe in detail how to train a classifier and

#### Algorithm 2 Prepare a classifier

**Input:** The dataset  $\mathcal{K}$ .

- 1: **Initialization:** Load the pre-trained feature extraction layer parameters of ResNet18 network, modify the output classes number of fully connection layer, then we can get the classification network's parameters  $W_{cla}$ .
- 2: **while** Stop criterion is not met **do**
- 3:   **Forward:**  $X \rightarrow \hat{Y} = F_X(X)$ ;
- 4:   **Loss:**  $\mathcal{L}_{cla} = \text{CE}(Y, \hat{Y})$ ;
- 5:   **Back-propagation:**  $\mathcal{L}_{cla} \rightarrow \frac{\partial \mathcal{L}_{cla}}{\partial W_{cla}}$ ;
- 6:   **Update parameters:**  $W_{cla} := W_{cla} - lr \frac{\partial \mathcal{L}_{cla}}{\partial W_{cla}}$
- 7: **end while**

**Output:** The parameterized network  $F_X$ .

#### Algorithm 3 Prepare a convolutional auto-encoder

**Input:** The dataset  $\mathcal{K}$ .

- 1: **Initialization:** Initialize the auto-encoder network's parameters  $W_{cae}$ .
- 2: **while** Stop criterion is not met **do**
- 3:   **Forward:**  $X \rightarrow \hat{X} = D_\phi(E_\theta(X))$ ;
- 4:   **Loss:**  $\mathcal{L}_{cae} = \text{MSE}(X, \hat{X})$ ;
- 5:   **Back-propagation:**  $\mathcal{L}_{cae} \rightarrow \frac{\partial \mathcal{L}_{cae}}{\partial W_{cae}}$ ;
- 6:   **Update parameters:**  $W_{cae} := W_{cae} - lr \frac{\partial \mathcal{L}_{cae}}{\partial W_{cae}}$
- 7: **end while**

**Output:** The parameterized network  $E_\theta$  and  $D_\phi$ .

an convolutional auto-encoder separately. The classifier is not trained from scratch, because we only need to get a standard classifier here. With the help of classic ResNet18 network, pre-trained feature extraction layer parameters can be preloaded, and then fine tuning training can be carried out to get a standard classification network. Auto-encoder is trained from scratch. See Algorithm 2 and Algorithm 3 for more details of these two training procedures.

#### Algorithm 4 Estimating Mutual Information $I(X; Z)$ Using CLUB method

**Input:** Dataset  $\mathcal{K}$ , fine-tuned auto-encoder  $E_\theta^*$ ,  $D_\phi^*$ .

- 1: **Initialization:** Initialize a variational network  $q_\xi(z|x)$  with parameters  $\xi$ .
- 2: **Collect variables  $X$  and  $Z$ :**  $X \rightarrow Z = E_\theta(X)$      $Z \rightarrow \hat{X} = D_\phi(Z)$      $\hat{X} \rightarrow \hat{Y} = F_X(\hat{X})$ ;
- 3: **while** Stop criterion is not met **do**
- 4:   **Sampling:** Sample  $\{(x_i, y_i)\}_{i=1}^N$  from  $p(x, z)$ ;
- 5:   **Forward:**  $X \rightarrow \mu, \sigma^2 \rightarrow \hat{Z}$ ;
- 6:   **Loss:**  $\mathcal{L}_{\text{CLUB}} = \text{MSE}(Z, \hat{Z})$ ;
- 7:   **Back-propagation:**  $\mathcal{L}_{\text{CLUB}} \rightarrow \frac{\partial \mathcal{L}_{\text{CLUB}}}{\partial W_{\text{CLUB}}}$ ;
- 8:   **Update parameters:**  $W_{\text{CLUB}} := W_{\text{CLUB}} - lr \frac{\partial \mathcal{L}_{\text{CLUB}}}{\partial W_{\text{CLUB}}}$
- 9: **end while**
- 10: **Estimating MI:**  $I_{\text{CLUB}} = \mathbb{E}_{p(x,y)} [\log q_\xi(y|x)] - \mathbb{E}_{p(x)} \mathbb{E}_{p(y)} [\log q_\xi(y|x)]$ .

**Output:** The estimating MI  $I_{\text{CLUB}}$ .

Algorithm 4 describes the steps of estimating mutual information provided by CLUB method. As we have analyzed in the previous section,  $Z$  and  $\hat{Y}$  are bottleneck variables. Following the information bottleneck principle, mutual information  $I(X; Z)$ ,  $I(Z; Y)$ , and  $I(X; \hat{Y})$ ,  $I(\hat{Y}; Y)$  are estimated using the



CLUB method. Though different MI need different estimating networks, these networks are similar to each other. We take  $I(X; Z)$  as an example to exhibit the computing process. See Algorithm 4 for further details.

Algorithm 5 describes the specific steps of transfer from classification task to object detection task. Our goal is to achieve a trade-off between prediction precision and generalization ability. Prediction precision means that reconstructed images can better complete the task using in the training stage. Generalization ability means that if the task on the receiver changes, the reconstructed image can still have a better performance on the changed task better. Here we take classification as the basic task and object detection as the target task. Note that **What we do is a simple transfer, the only change is the task at the receiver, and we doesn't further train the convolutional auto-encoder, which means that the network parameters used in the transfer experiments are the same as the fine tuning trained network with classification task.**

**Algorithm 5** Transfer testing: from classification to object detection

**Input:** The dataset  $\mathcal{K}$ , fine-tuned auto-encoder  $E_\theta^*$ ,  $D_\phi^*$  and pretrained object detection network  $T_\psi$ .

- 1: **Test with normal auto-encoder:**  $X \rightarrow \hat{X} = D_\phi(E_\theta(X))$   
 $\hat{X} \rightarrow \hat{Y} = T_\psi(\hat{X});$
- 2: **Test with fine-tuned auto-encoder:**  $X \rightarrow \hat{X}^* = D_\phi^*(E_\theta^*(X))$   
 $\hat{X}^* \rightarrow \hat{Y}^* = T_\psi(\hat{X}^*);$
- 3: Compare the mAP performance of  $\hat{Y}$  and  $\hat{Y}^*$

**Output:** The transfer performance.

## V. EXPERIMENTS

In this section, we provide extensive experiments to show the effectiveness of semantic image communication system. These experiments consist of four parts. First, we compare the proposed method with traditional and DNN-based methods in terms of the performance of prediction and reconstruction under different bpp and SNR. Second, several mutual information are estimated to verify the assumption that, the loss function we actually used has close relationships with mutual information. On the other hand, the changes of the these mutual information also can be used to explain the changes of performance in the first part of experiments. Then, in order to demonstrate the generalization among different task of the proposed method, we test the transfer performance from classification to object detection. Finally, the impacts of parameter  $\beta$  are explored, **which shows that the trade-off between  $D_{RD}$  and  $D_{IB}$  is necessary.**

### A. Simulation settings

1) **Datasets:** In our experiments, STL10 dataset is adopted for classification, and Pascal VOC 2007 dataset is adopted for object detection.

The STL-10 dataset is an image recognition dataset for developing deep learning algorithms. Specifically, there are 100000 unlabeled images for unsupervised learning. The image size is  $96 \times 96$ . For supervised learning, it has 10 classes, each class has 500 training images and 800 test images with labels. Since our method is semi-supervised, we mainly utilize the labeled images for training and testing.

The Pascal VOC 2007 dataset provides standardised image data sets for object class recognition. The dataset includes 9,963 images split into train/test sets which separately include 5,011 and 4,952 images. We use our pretrained image communication system to transmitting the test set and use the mature detection models to measure the mAP.

TABLE I  
THE NETWORK SETTINGS.

|                  | Layer Name       | Layer   | Activation |
|------------------|------------------|---|------------|
| Encoder          | Conv1            | 128x8x8, stride 4                               | Relu       |
|                  | ResBolck1        | 128x3x3, stride 1<br>128x3x3, stride 1          | Relu       |
|                  | Conv2            | 256x4x4, stride 2                               | Relu       |
|                  | ResBolck2        | 128x3x3, stride 1<br>256x3x3, stride 1          | Relu       |
|                  | ResBolck3        | 128x3x3, stride 1<br>256x3x3, stride 1          | Relu       |
|                  | Conv3            | $K \times 3 \times 3$ , stride 1                | Sigmoid    |
| Quantizer        | Binary Quantizer | Forward: $z = [e]$<br>Backprop: $\tilde{z} = e$ | None       |
| Channel          | AWGN             | $\tilde{z} = z + n$                             | None       |
| Decoder          | Conv4            | 512x1x1   | Relu       |
|                  | ResBolck4        | 128x3x3, stride 1<br>512x3x3, stride 1          | Relu       |
|                  | ResBolck5        | 128x3x3, stride 1<br>512x3x3, stride 1          | Relu       |
|                  | Up-Sampling1     | DepthToSpace(2)                                 | None       |
|                  | Conv5            | 256x3x3, stride 1                               | Relu       |
|                  | ResBolck2        | 128x3x3, stride 1<br>256x3x3, stride 1          | Relu       |
|                  | Up-Sampling2     | DepthToSpace(4)                                 | None       |
|                  | Conv6            | 32x3x3, stride 1                                | Relu       |
|                  | Conv7            | 3x3x3, stride 1                                 | None       |
| Classifier       | ResNet-18        | Default   | None       |
| Object Detection | RFBNet           | Default   | None       |
| MI Model         | Linear1          | 1024  | Relu       |
|                  | Linear2          | 512   | Relu       |
|                  | Linear3          | 512   | Relu       |
|                  | Linear4          | dimension of $z$                                | None       |

TABLE II  
THE TRAINING HYPER-PARAMETERS SETTINGS.

|                          | Classifier | CAE                           | SICS               | MI Model  |
|--------------------------|------------|-------------------------------|--------------------|-----------|
| Learning Rate            | $10^{-3}$  | $10^{-4} \rightarrow 10^{-6}$ | $3 \times 10^{-6}$ | $10^{-4}$ |
| Epochs                   | 1000       | 5000                          | 1000               | 1000      |
| Batch Size               | 16         | 32                            | 32                 | 200       |
| Weight Decay             | None       | $10^{-5}$                     | $10^{-5}$          | None      |
| Trade-Off Factor $\beta$ | None       | None                          | $(0, \infty)$      | None      |
| SNR(dB)                  | None       | None                          | $[-5, 20]$         | None      |

2) **Network and Hyper-parameters:** As shown in algorithm 1, The proposed semantic image communication system requires pretrained classifier and auto-encoder. We adopt the classic ResNet-18 network as our classifier, and construct a specialized auto-encoder. After training these two networks until convergence according to algorithm 2 and 3 respectively, we can further achieve our method by algorithm 1. Leveraging algorithm 4 and a variational approximation mappings, mutual information can be estimated. Algorithm 5 shows the processing of transfer experiment.

The specific settings about various networks can be found in Table I. Note that the encoder performs down-sampling while implementing the convolutional operation by setting the stride to different number, while in the decoder, up-sampling is performing by depth-to-space operation. Besides, in the forward propagation, the rounding operation is executed in the binary quantizer, where  $[\cdot]$  is defined as rounding. In addition, The network structures of classifier and objection detection are default settings of ResNet-18 and RFBNet, exception the fully connected layer in the ResNet-18, which is modified to 10 dimensions to adapt the practical task. Finally, the MI model

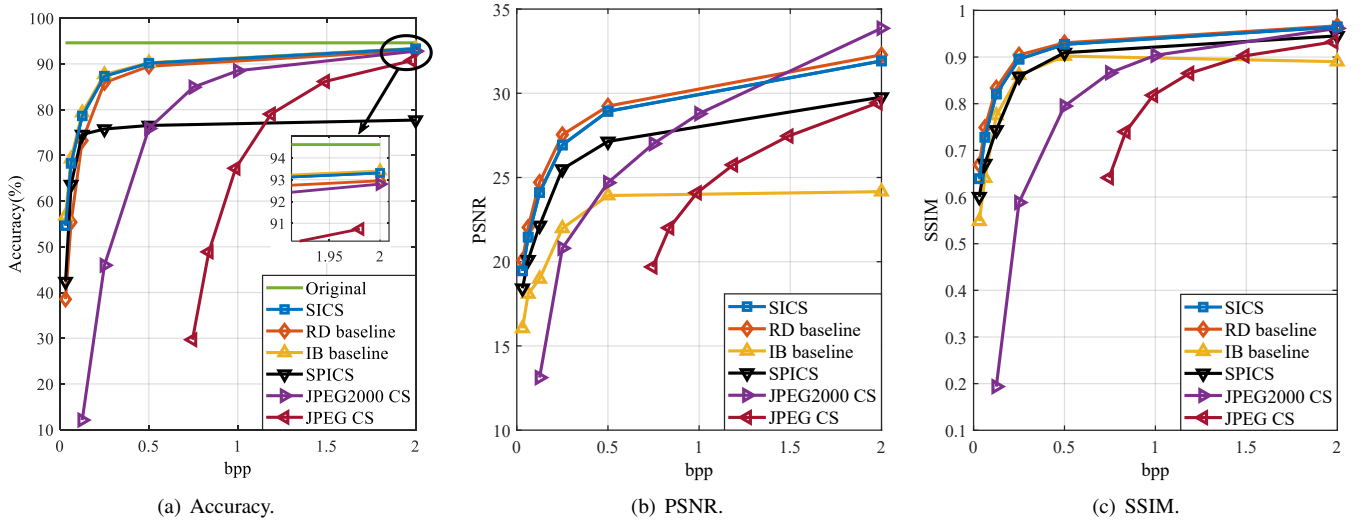


Fig. 4. Comparisons of different methods with respect to the performance of classification and reconstruction under different bpp with  $\text{SNR} = \infty$ ,  $\beta = 0.01$ . The performance of classification is assessed by classification accuracy, and the performance of reconstruction is assessed by PSNR and SSIM.

is a variational network, which is to approximate the mappings between two variables.

The training parameters in algorithm 1 to 4 are shown in Table II. Note that SICS is trained based on the separate classifier and CAE, so the learning rate is lower. The batch size of MI model is set to 200 due to this model need rich data to reduce the estimation error. The trade-off factor  $\beta$  and SNR only exist in our proposed SICS.

**Since the CAE's structure we adopted here is not the state of art, its performance of reconstruction can be better if we choose the more complex structure. In order to show the improvement more clearly, we didn't adopt the state of art structure.**

**3) Comparison Methods:** We compare the proposed SICS with the traditional and other DNN-based image communication systems.

In traditional image communication system, image is firstly compressed by JPEG or JPEG2000 method, then transmitted to the receiver, and reconstructed by the corresponding decoder. The encoder and decoder are both typically manual-designed. Finally, specific intelligend task takes these images as input to complete the application. We refer the traditional method as JPEG communication system (JPEG CS) and JPEG2000 communication system (JPEG2000 CS).

The most closely related to our method are the works of Sihui Luo's [31] and Neel Patwa's [4]. They placed a fully-connected neural network right after the encoder to perform classification, which means that the encoder is also the feature extractor of the classifier, and the classification and reconstruction are implemented simultaneously. To make fair comparison, the structures of the auto-encoder used in our and their method are same. And we refer their method as semantic-preserving image communication system (SPICS).

In order to show the effectiveness of our method more directly, we also presented the performance of RD baseline and IB baseline. RD baseline means that setting  $\beta$  to zero, i.e. ignoring the  $D_{IB}$ , then our method degrades to the general image communication system optimizing for perception quality of images. IB baseline means that setting the optimizing object to  $D_{IB}$ , i.e. ignoring the  $D_{RD}$ . Then our method becomes the standard information bottleneck optimization.

## B. Comparison Experiments

**1) Performance versus bpp:** Fig.4 shows the comparisons of different methods with respect to the performance of clas-

sification and reconstruction under different bpp with  $\text{SNR} = \infty$ ,  $\beta = 0.01$ . **In order to avoid the model's fluctuation, we took the average of the final five classification accuracy rates, PSNRs and SSIMs of validation set.** The classification accuracy for original images is 94.61%. In the following analysis, we consider the classification accuracy and reconstruction quality jointly.

We first compare the proposed SICS with traditional methods (JPEG and JPEG2000). Fig.4(a) shows that the SICS outperforms the JPEG and JPEG2000 CS in terms of classification performance under all bpp settings, especially in the low bpp. Fig.4 (b) and (c) show that the SICS is superior or competitive to traditional methods in terms of the reconstruction performance, which is consistent with the opinion of most DNN-based image compression methods [10], [11], [12]. In essence, it is the better quality of reconstruction images that leads to better classification performance.

Then compare the proposed SICS with SPICS [4]. Fig.4 shows that SICS outperforms SPICS both in terms of classification and reconstruction performance under the same CAE networks and hyperparameters. These improvements should be attributed to the cascade structure shown in Fig.3. SPICS is actually a multi-task learning model, which results that the performance in each task can't exceed single-task optimization case due to the different learning objectives between the tasks. While thanks to the cascade structure, our proposed SICS don't suffer from this problem. In general, the task performance is almost positively related to the quality of reconstruction. Besides, cascade structure is more flexible because of the networks of auto-encoder and task are decouple. So we can take advantage of various mature-pretrained task networks, i.e., making full use of transfer learning by fine-tuning these pretrained networks, which is impossible for the structure in [4]. **When the target dataset is significantly smaller than the base dataset, transfer learning can be a powerful tool to enable training a large target network without overfitting [42].**

Observing the comparisons between SICS and two baselines. Fig.4 shows that IB baseline attained the best classification performance, while the quality of reconstruction drops a lot compared with RD baseline and SICS, **which will weaken the generalization ability among different tasks**, i.e., these reconstructed images are unable to perform other tasks well. This will be further discussed in the later experiments. On the other hand, observing the RD baseline. Though it achieves

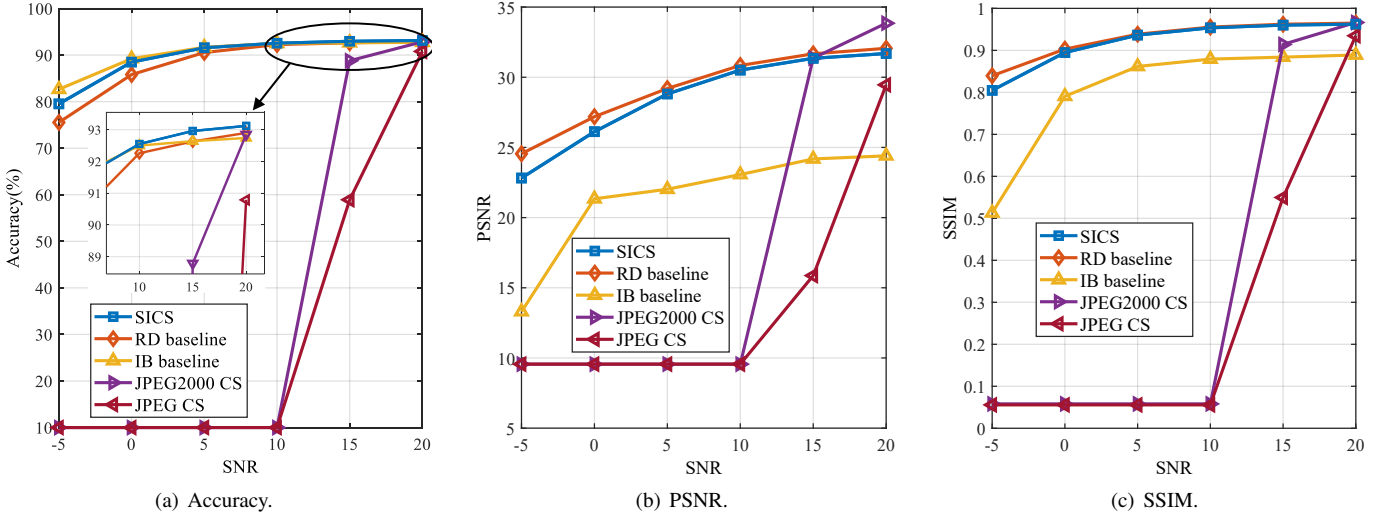


Fig. 5. Comparisons of different methods with respect to the performance of classification and reconstruction under different SNR with  $\text{bpp} = 2$ ,  $\beta = 0.01$ . The performance of classification is assessed by classification accuracy, and the performance of reconstruction is assessed by PSNR and SSIM.

the best quality of reconstruction, the classification performance is inferior to SICS, which support our hypothesis that perceptual-significant visual features may not be the most suitable for intelligent task. **In practice, in a semantic communication system with a large number of agents, it's better to reconstruct the images more suitable for the AI agent's task.** The SICS achieved an ideal trade-off between predictive precision and generalization ability compared to RD baseline by improving the reconstructed image's predictive precision in classification task **at the expense of a small amount of perception quality.**

2) *Performance versus SNR*: Fig.5 shows the comparisons of different methods with respect to the performance of classification and reconstruction under different SNR with  $\text{bpp} = 2$ ,  $\beta = 0.01$ . Here we compare the SICS with traditional methods and two baselines.

Observing the performance of JPEG CS and JPEG2000 CS, there appears abrupt performance degradations in certain SNR, known as the "cliff effect" in digital communication. The "cliff effect" means that the performance falls off steeply until to the worst levels when the channel condition is lower than a certain threshold. As shown in the [?], DNN-based joint source and channel coding algorithms can overcome the "cliff effect". Here, our proposed SICS also don't suffer from it, specifically, as the SNR decreases, the classification and construction performances of SICS decrease slowly.

Comparing SICS with RD and IB baselines. Fig.5(a) shows that the SICS is superior to RD baseline but inferior to IB baseline in terms of classification performance. And the IB baseline is exceeded by the SICS in the high SNRs. On the contrary, Fig.5(b) and (c) show that the SICS is superior to IB baseline by a significant margin but slightly inferior to RD baseline in terms of reconstruction performance. This phenomenon implies that, once again, the SICS achieved an ideal trade-off between predictive precision and generalization ability compared to RD baseline by improving the reconstructed image's predictive precision in classification task **at the expense of a small amount of perception quality.**

### C. Mutual Information Estimation Results

Why is it that the best appearance images are not necessarily the best ones for the classification task? This needs to be explained from the perspective of information theory.

According to the previous analysis, variables  $Z$  and  $\hat{Y}$  are two critical variables in the whole end-to-end communication

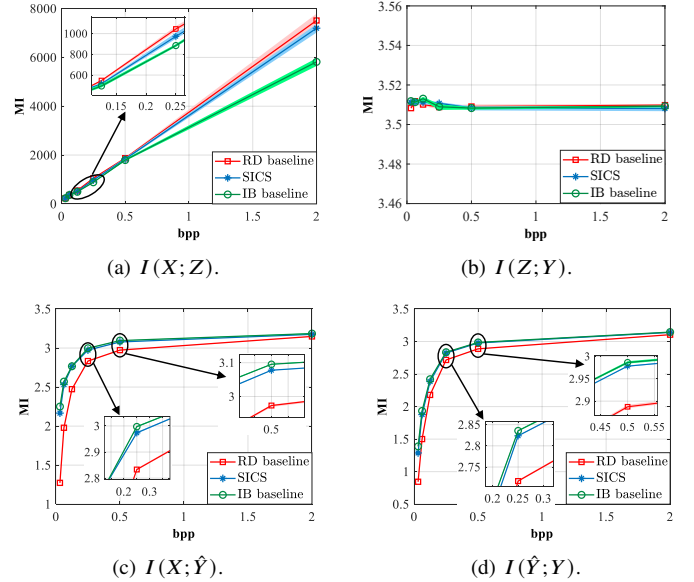


Fig. 6. Comparisons of different methods with respect to four MI,  $I(X; Z)$ ,  $I(Z; Y)$ ,  $I(X; \hat{Y})$ , and  $I(\hat{Y}; Y)$  under different  $\text{bpp}$  with  $\text{SNR} = \infty$ ,  $\beta = 0.01$ .

link. In this section we mainly estimate these MI values among SICS, RD baseline and IB baseline. In line with information bottleneck method, we estimated the mutual information of intermediate variables with input variable and desired output variable, respectively, namely  $I(X; Z)$ ,  $I(Z; Y)$ ,  $I(X; \hat{Y})$ , and  $I(\hat{Y}; Y)$ . The physical meanings of these four MI are described below.

$I(X; Z)$ , the mutual information of the auto-encoder's information bottleneck variable  $Z$  and the input  $X$ , represents the amount of information relevant to  $X$  contained in  $Z$ . This value shows that, on the one hand, how much information relevant to  $X$  is retained after encoding. On the other hand, it reflects the compression of  $Z$  with respect to  $X$ . The smaller this MI value, the greater compression degree.

$I(Z; Y)$ , the mutual information of the auto-encoder's information bottleneck variable  $Z$  about the desired output  $Y$ , represents the amount of information about  $Y$  contained in  $Z$ ,

which reflects the potential of  $Z$  to perform the task. The greater this MI value, the more information about the label  $Y$  captured by  $Z$ ;

$I(X; \hat{Y})$ , the mutual information of classifier's bottleneck variable  $\hat{Y}$  and input  $X$ , represents the amount of information about  $X$  contained in  $\hat{Y}$ .

$I(\hat{Y}; Y)$ , the mutual information of the classifier's information bottleneck variable  $\hat{Y}$  and desired output  $Y$ , represents the amount of information relevant to  $Y$  contained in  $\hat{Y}$ , which reflects the potential of  $\hat{Y}$  to perform the task. The larger the value is, the more information about  $Y$  is captured by  $\hat{Y}$ .

Fig.6 shows the comparisons of different methods in terms of four mutual information. Since the CLUB method produces different values within a certain range each estimation, we estimate mutual information multiple times and compute the maximal, minimal and mean values. Then we draw the region bounded by the maximal and minimal values in light colors and plot the corresponding mean values in dark colors. These estimating results yield many findings listed as following.

- **The loss functions we actually used in different methods have close relationships with mutual information.** From Fig.6 (a) we can find that, RD baseline, adopted the MSE-only objective, produced the maximal  $I(X; Z)$ , since minimizing  $MSE(X; \hat{X})$  is equivalent to maximizing  $I(X; Z)$ . SICS, optimized for MSE and  $D_{IB}$  trade-off objective, exhibited a slightly smaller  $I(X; Z)$ , since the influence of  $D_{IB}$ . IB baseline showed the minimal  $I(X; Z)$  because the  $D_{IB}$  is the only objective, and minimizing  $D_{IB}$  means maximizing  $I(\hat{Y}; Y)$ , which is different from  $I(X; Z)$ . On the contrary, from Fig.6 (d) we can find that, RD baseline produced the minimal  $I(\hat{Y}; Y)$ , IB baseline produced the maximal values, and the values of SICS is slightly lower than IB baseline. This phenomenon is also resulted by the different settings of optimization objectives.
- **The changes of mutual information result in the changes of performance of classification and reconstruction.** Observing the changes of mutual information in Fig.6 (a) (d) and performance of different tasks, we can find that, they have the consistent trend. The maximal  $I(X; Z)$  and minimal  $I(\hat{Y}; Y)$  of RD baseline correspond to the best reconstruction performance and worst classification performance. The minimal  $I(X; Z)$  and maximal  $I(\hat{Y}; Y)$  of IB baseline correspond to the worst reconstruction performance and best classification performance. Finally, the median MI values of SICS correspond to medium performance of different tasks. These results show that proper trade-off between different optimization objectives can reach both satisfactory performance of various tasks.
- **Fig.6 (b) shows the comparisons of different methods in terms of  $I(Z; Y)$ .**  $I(Z; Y)$  is not included in our optimization objective. From the results we can find that the three methods have almost the same values of  $I(Z; Y)$ , and the values is located around 3.51. Note that  $I(Z; Y) = H(Y) - H(Y|Z) \leq H(Y) = \log_2(10) \approx 3.3219$ . So the estimations of  $I(Z; Y)$  have saturated. It is bigger than  $\log_2 10$  because the CLUB produced the upper bound of mutual information. Since the most of information contained in  $Z$  is relevant to  $X$ , **though  $I(Z; Y)$  is large enough, the redundant information about  $X$  will affect the classification performance.**
- **Fig.6 (c) shows the comparisons of different methods in terms of  $I(X; \hat{Y})$ .**  $I(X; \hat{Y})$  is also not included in our optimization objective. And  $\hat{Y}$  is the bottleneck variable of classification network. Through the classification network,  $\hat{Y}$  tried to discard as much information relevant to  $X$  as possible, and retain as much information relevant to  $Y$

as possible. **So  $I(X; \hat{Y})$  in different methods have the similar variation trends.**

If the distorted description is merely  $D_{RD}$ , which is actually MSE here, then this pixel-by-pixel approach is equivalent to preserving as much feature information as possible of the original image without discriminating and any trade-off. However, we believe that in the case of limited bit rate, if the image is still recovered with MSE as the target, it is not beneficial to the execution of downstream intelligent tasks. In specific, the network is no longer able to recover the original image well in the low bit rate. **If you insist on recovering the image pixel-by-pixel, it will become less recognizable.**

If the description of distortion is only  $D_{IB}$ , which is, the loss of mutual information  $I(\hat{X}; Y)$  is taken as the distortion in the way of information bottleneck, this is equivalent to a certain selection of recovered features. In this way, the recovered  $\hat{X}$  will retain as much as possible of the feature information relevant to corresponding task. **Although this is good for the task, the structural information of the original image is completely destroyed, making it impossible to perform other tasks, especially those tasks need the structural information, and in fact, it is almost impossible to reconstruct the a meaningful image for human eyes.**

According to our method, the loss of two kinds of distortion, MSE and mutual information  $I(\hat{X}; Y)$ , is weighted into consideration, so that the task-related feature information can be selectively recovered, and some generalization performance can be retained. In the case of limited bit rate, it not only ensures the performance of completing the task, but also enables the network to reconstruct the image with slightly reduced quality. At this time, the reconstructed image has already contained more feature information related to the task, which is called semantic reconstruction.

The above analysis of our experimental results is from the perspective of information theory. **In essence, both our method and ordinary auto-encoders reconstruct images, but they follow different distortion functions.** Finally, we will try to understand the difference between proposed method and baseline **from a more intuitive perspective.** That is, directly observe the images reconstructed by the two methods.

## Appendix C

### D. Transfer experiments

Fig. 7 shows the transfer performance of different methods from classification to object detection. **Note that RFBNet's mAP on the original Pascal VOC 2007 test dataset is 80.67%.** Observing Fig. 7 (a) we can find that, In contrast to the classification task case, here SICS exhibit the best performance among these three methods. IB baseline is even inferior to RD baseline in terms of mAP. Fig. 7 (b) and (c) show the similar relationships as in previous basic experiments in terms of reconstruction quality.

**According the above results we can believe that, the trade-off factor  $\beta$  plays a critical role in ensuring good generalization ability.** Though IB baseline exhibited the better classification performance than SICS in the previous experiments, the following experiment results will show that, the images reconstructed by IB baseline show poor generalization on a different task, which means that when the semantic auto-encoder is transferred to another system with any other tasks except classification, its performance will drop quickly.

On the other hand, the performance improvement of object detection is not as large as that of classification, which increases with the decrease of bpp. This is because what we did was just a simple transfer test, and the model trained by STL10 classification was directly applied to the object detection task. At this time, there was no joint training between the auto-encoder network and the object detection network, and there

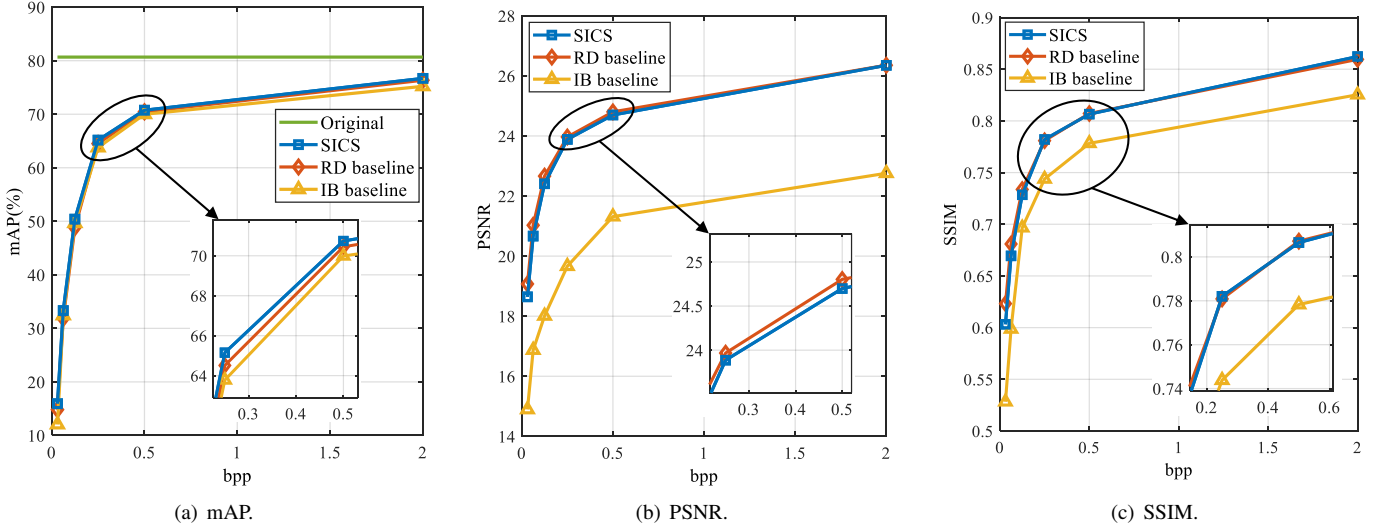


Fig. 7. Comparisons of different methods with respect to the performance of object detection and reconstruction under different bpp with  $\text{SNR} = \infty$ ,  $\beta = 0.01$ . The performance of object detection is assessed by mAP, and the performance of reconstruction is assessed by PSNR and SSIM.

may be a mismatch between the two networks (The distribution of the data reconstructed by the auto-encoder has changed, while the object detection network is a fixed model after the training of the original image data set). **If we combine the auto-encoder and the object detection network for fine-tuning training, the performance may be further improved. That's our future work.**

#### Appendix C

**When the semantic auto-encoder trained by the classification task are applied to the scene of object detection, the performance is also improved steadily. This is surprising and remarkable, and it can be explained.** When we are training the basic semantic image transmission model, while using the distortion and MSE weighted and classification task, but the classification task itself is a more basic intelligence task, there is reason to believe that this is because the classification distortion makes the model in the reconstructed image and keep the semantic features of the image information as much as possible, which leads to the improvement of object detection performance.

**consequently, if the target task in the receiver is decided and changeless, we'd better use the IB baseline. But in practice, the receiver has to handle multiple tasks, in order to ensure that the reconstructed images can perform these tasks well simultaneously, SICS is the better choice.**

#### E. Impact of Trade-off Factor $\beta$

Essentially, the only difference between SICS, RD baseline and IB baseline is  $\beta$ , which is the trade-off factor between  $D_{RD}$  and  $D_{IB}$ . In the previous experiments,  $\beta$  in SICS is fixed to 0.01 for proper performances. What's more, we have intuitively seen the powerful effect of  $\beta$ , and Fig. 7 shows that, IB baseline is inferior to SICS in terms of both performance of task and reconstruction, which shows that IB baseline has poor transfer performance. From RD baseline to IB baseline,  $\beta$  is monotonically increasing. In this section, we explore the dynamics of performance as  $\beta$  increases from 0 to  $\infty$ .

Fig. 8 shows the performance's dynamics of source and target tasks in terms of trade-off factor  $\beta$ . We first observe the source task's dynamics. Fig. 8 (a) shows that the classification accuracy gets improved as  $\beta$  increases, and the growth rate is getting slower and slower. Meanwhile, this promotion is limited by the case of  $\beta = \infty$ , from our training curves, the accuracy

has reached the plateau. Fig. 8 (b) and (c) show that the quality of reconstruction is getting worse and worse as  $\beta$  increases, and it's going down faster. Meanwhile, this deterioration is unlimited, from the training curves, the perceptual quality will go further down as the training iterations increase. Unlike the classification task, Fig. 8 (a) shows that the mAP of object detection task exhibits a trend of increase first and then decrease. Fig. 8 (b) and (c) show that both tasks perform similar dynamics of reconstruction performance.

There are several interesting phenomenon need to explain. First, source and target tasks show different dynamics in terms of precision, the reason is that we directly transferred the system trained on classification task to object detection task without further training the semantic auto-encoder for object detection. When  $\beta$  increases at first, our semantic auto-encoder can extract and remain the general semantic features, which is beneficial to various intelligent tasks. But as  $\beta$  goes up beyond a threshold, the semantic auto-encoder will extract and remain the features specific to classification tasks, which results the degradation of performance of target task, i.e. mAP. Second, the reconstruction performance of Pascal VOC2007 is always inferior to STL10. This is also because we train the SICS with STL10 dataset, and these two datasets differ greatly in both image size and style. We believe the performance will get improved if the Pascal VOC dataset is used to train the SICS.

#### VI. CONCLUSION

In this paper, we proposed a semantic image communication system based on the extended rate-distortion theory, **which is jointly optimized for the predicting precision and generalization ability among different intelligent tasks of the reconstructed images.** Specifically, we extended the rate-distortion theory by taking the trade-off between reconstruction distortion and task distortion as the semantic distortion, and further designed the semantic image communication system based on the widely used auto-encoder architecture followed by the task network. **We also noted that, the semantic distortion we define here is closely related to mutual information, which means that our semantic communication system can be explained from the information theoretic view.** The simulation results have shown that the proposed method outperforms the traditional and DNN-based methods in both classification and object detection tasks under different bpp and SNR. And the mutual information estimation results show that



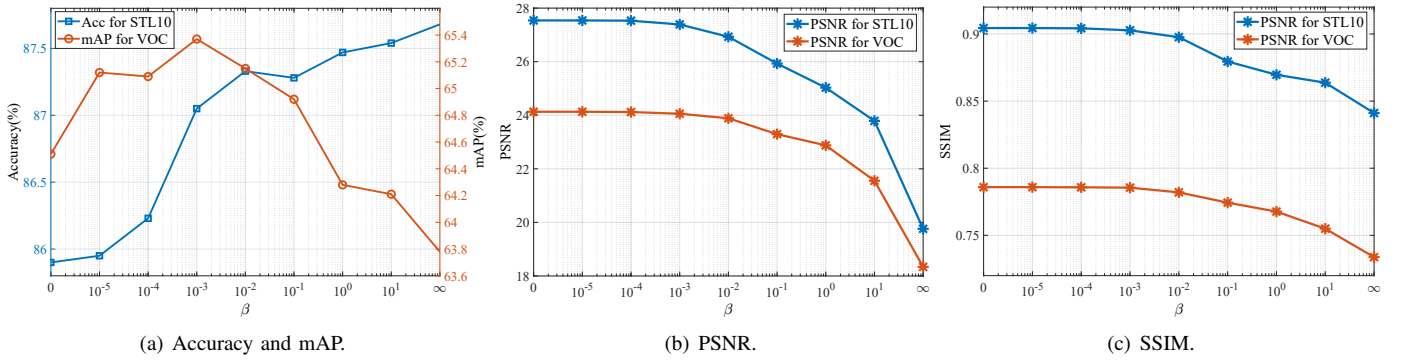


Fig. 8. Comparisons of different tasks and datasets with respect to the performance of precision and reconstruction under different  $\beta$  with  $\text{bpp} = 0.25$ ,  $\text{SNR} = \infty$ . The classification performance is assessed by accuracy, the object detection performance is assessed by mAP, and the performance of reconstruction is assessed by PSNR and SSIM.

our SICS indeed extract more semantic information. Therefore our proposed method can be useful in IoT communication with various intelligent tasks need to perform.

## APPENDIX A

In this section we will prove that the relevant information distortion functions used in this paper are equivalent.

Denote  $d_{IB}(x, \hat{x})$  as the relevant information distortion between  $x$  and  $\hat{x}$ ,

$$d_{IB}(x, \hat{x}) = \sum_y p(y|x) \log \left( \frac{p(y|x)}{p(y|\hat{x})} \right) \quad (35)$$

Denote  $D_{IB}(X, \hat{X})$  as the expectation of relevant information distortion between  $X$  and  $\hat{X}$ ,

$$D_{IB}(X, \hat{X}) = E[d_{IB}(x, \hat{x})] = \sum_x \sum_y p(y|x) \log \left( \frac{p(y|x)}{p(y|\hat{x})} \right) \quad (36)$$

We first prove conditional mutual information  $I(X; Y|\hat{X})$  does describe the relevant information distortion. According to the markov chain  $Y \rightarrow X \rightarrow \hat{X}$ ,

$$p(y|x, \hat{x}) = p(y|x) \quad (37)$$

According to the definition of conditional mutual information, and implement equation (37)

$$\begin{aligned} I(X; Y|\hat{X}) &= \sum_{\hat{x}} \sum_x \sum_y p(\hat{x}) p(x, y|\hat{x}) \log \left( \frac{p(x, y|\hat{x})}{p(x|\hat{x}) p(y|\hat{x})} \right) \\ &= \sum_{\hat{x}} \sum_x \sum_y p(\hat{x}) p(x, y|\hat{x}) \log \left( \frac{p(y|x, \hat{x}) p(x|\hat{x})}{p(x|\hat{x}) p(y|\hat{x})} \right) \\ &= \sum_{\hat{x}} \sum_x \sum_y p(\hat{x}) p(y|x, \hat{x}) p(x|\hat{x}) \log \left( \frac{p(y|x)}{p(y|\hat{x})} \right) \\ &= \sum_{\hat{x}} \sum_x \sum_y p(x, \hat{x}) p(y|x) \log \left( \frac{p(y|x)}{p(y|\hat{x})} \right) \\ &= D_{IB} = E[d_{IB}(x, \hat{x})] \end{aligned} \quad (38)$$

Then we prove

$$I(X; Y) - I(\hat{X}; Y) = I(X; Y|\hat{X}) \quad (39)$$

According to the definition of mutual information,

$$\begin{aligned} I(X; Y) - I(\hat{X}; Y) &= \sum_x \sum_y p(x, y) \log \left( \frac{p(x, y)}{p(x)p(y)} \right) \\ &\quad - \sum_{\hat{x}} \sum_y p(\hat{x}, y) \log \left( \frac{p(\hat{x}, y)}{p(\hat{x})p(y)} \right) \\ &= \sum_{\hat{x}} \sum_x \sum_y p(\hat{x}, x, y) \log \left( \frac{p(x, y)}{p(x)p(y)} \right) \\ &\quad - \sum_{\hat{x}} \sum_x \sum_y p(\hat{x}, x, y) \log \left( \frac{p(\hat{x}, y)}{p(\hat{x})p(y)} \right) \\ &= \sum_{\hat{x}} \sum_x \sum_y p(\hat{x}, x, y) \log \left( \frac{p(y|x)}{p(y)} \right) \\ &\quad - \sum_{\hat{x}} \sum_x \sum_y p(\hat{x}, x, y) \log \left( \frac{p(y|\hat{x})}{p(y)} \right) \\ &= \sum_{\hat{x}} \sum_x \sum_y p(\hat{x}, x, y) \log \left( \frac{p(y|x)}{p(y|\hat{x})} \right) \\ &= D_{IB} = E[d_{IB}(x, \hat{x})] \end{aligned} \quad (40)$$

## APPENDIX B

In this section we give the proof of equation 10. Rewrite the optimization problem (9) as follows:

$$\min_{\substack{p(\hat{x}|x): I(X, \hat{X}) \leq I_C \\ \sum_{\hat{x}} p(\hat{x}|x) = 1}} D_{RD}(X, \hat{X}) - \beta I(\hat{X}; Y) \quad (41)$$

Using the Lagrange multiplier method by first formulating the Lagrange functional,

$$\begin{aligned} \mathcal{L}(p(\hat{x}|x)) &= \lambda I(X; \hat{X}) + D_{RD}(X; \hat{X}) - \beta I(\hat{X}; Y) \\ &\quad + \sum_x r(x) \sum_{\hat{x}} p(\hat{x}|x) \\ &= \lambda \sum_x \sum_{\hat{x}} p(x) p(\hat{x}|x) \log \frac{p(\hat{x}, x)}{p(\hat{x})} \\ &\quad + \sum_x \sum_{\hat{x}} p(x) p(\hat{x}|x) d_{RD}(x, \hat{x}) \\ &\quad - \beta \sum_{\hat{x}} \sum_y p(y) p(\hat{x}|y) \log \frac{p(\hat{x}, y)}{p(\hat{x})} \\ &\quad + \sum_x r(x) \sum_{\hat{x}} p(\hat{x}|x) \end{aligned} \quad (42)$$



where  $\lambda$  is the Lagrange multiplier attached to the constrained  $I(X; \hat{X})$ ,  $r(x)$  is the Lagrange multiplier attached to the normalization of the mapping  $p(\hat{x}|x)$  for corresponding  $x$ .

According to the Markov chain  $Y \leftrightarrow X \leftrightarrow \hat{X}$ , we get  $p(\hat{x}|x, y) = p(\hat{x}|x)$  and  $p(y|x, \hat{x}) = p(y|x)$ , then

$$p(\hat{x}) = \sum_x p(x)p(\hat{x}|x) \quad (43)$$

$$\begin{aligned} p(\hat{x}|y) &= \sum_x p(\hat{x}, x|y) \\ &= \sum_x p(\hat{x}|x, y)p(x|y) \\ &= \sum_x p(\hat{x}|x)p(x|y) \end{aligned} \quad (44)$$

from equations (43) and (44), we can get the derivatives w.r.t.  $p(\hat{x}|x)$

$$\frac{\partial p(\hat{x})}{\partial p(\hat{x}|x)} = p(x) \quad (45)$$

$$\frac{\partial p(\hat{x}|y)}{\partial p(\hat{x}|x)} = p(x|y) \quad (46)$$

Taking derivatives of (9) with respect to  $p(\hat{x}|x)$  for given  $x$  and  $\hat{x}$

$$\begin{aligned} \frac{\partial \mathcal{L}(p(\hat{x}|x))}{\partial p(\hat{x}|x)} &= \lambda p(x) \log \frac{p(\hat{x}|x)}{p(\hat{x})} + \lambda p(x)p(\hat{x}|x) \frac{1}{p(\hat{x}|x)} \\ &\quad - \lambda \sum_x p(x)p(\hat{x}|x) \frac{p(x)}{p(\hat{x})} + p(x)d_{RD}(x, \hat{x}) \\ &\quad - \beta \sum_y \frac{\partial p(\hat{x}|y)}{\partial p(\hat{x}|x)} p(y)[1 + \log p(\hat{x}|y)] \\ &\quad + \beta \frac{\partial p(\hat{x})}{\partial p(\hat{x}|x)} [1 + \log p(\hat{x})] + r(x) \end{aligned} \quad (47)$$

substitute (45) and (46) into (47)

$$\begin{aligned} \frac{\partial \mathcal{L}(p(\hat{x}|x))}{\partial p(\hat{x}|x)} &= \lambda p(x) \log \frac{p(\hat{x}|x)}{p(\hat{x})} + p(x)d_{RD}(x, \hat{x}) \\ &\quad - \beta \sum_y p(x, y)[1 + \log p(\hat{x}|y)] \\ &\quad + \beta p(x)[1 + \log p(\hat{x})] + r(x) \end{aligned} \quad (48)$$

rearranging this equation

$$\begin{aligned} \frac{\partial \mathcal{L}(p(\hat{x}|x))}{\partial p(\hat{x}|x)} &= \lambda p(x) \left[ \log \frac{p(\hat{x}|x)}{p(\hat{x})} + \lambda^{-1} d_{RD}(x, \hat{x}) \right] \\ &\quad - \beta p(x) \left[ \sum_y p(y|x) \log \frac{p(y|\hat{x})}{p(y)} \right] + r(x) \end{aligned} \quad (49)$$

Notice that  $\sum_y p(y|x) \log \frac{p(y|\hat{x})}{p(y)} = I(x; Y)$  is a function of  $x$  only (independent of  $\hat{x}$ ), and thus can be absorbed into the multiplier  $r(x)$ . Introducing

$$\log \mu(x) = \frac{1}{\lambda} \left( \frac{r(x)}{p(x)} - \beta \sum_y p(y|x) \log \frac{p(y|\hat{x})}{p(y)} \right)$$

finally, (49) can be simplified to

$$\begin{aligned} \frac{\partial \mathcal{L}(p(\hat{x}|x))}{\partial p(\hat{x}|x)} &= \lambda p(x) \left[ \log \frac{p(\hat{x}|x)}{p(\hat{x})} + \lambda^{-1} d_{RD}(x, \hat{x}) \right] \\ &\quad - \beta p(x) \left[ \sum_y p(y|x) \log \frac{p(y|\hat{x})}{p(y)} \right] \\ &\quad + \beta p(x) \left[ \sum_y p(y|x) \log \frac{p(y|x)}{p(y)} \right] \\ &\quad - \beta p(x) \left[ \sum_y p(y|x) \log \frac{p(y|x)}{p(y)} \right] + r(x) \\ &= \lambda p(x) \left[ \log \frac{p(\hat{x}|x)}{p(\hat{x})} + \lambda^{-1} d_{RD}(x, \hat{x}) \right] \\ &\quad + \beta p(x) \left[ \sum_y p(y|x) \log \frac{p(y|x)}{p(y|\hat{x})} \right] \\ &\quad + \lambda p(x) \log \mu(x) \end{aligned} \quad (50)$$

we know that

$$\begin{aligned} d_{IB}(x, \hat{x}) &= D_{KL}[p(y|x)||p(y|\hat{x})] \\ &= \sum_y p(y|x) \log \frac{p(y|x)}{p(y|\hat{x})} \end{aligned} \quad (51)$$

and set (50) to zero,

$$p(\hat{x}|x) = \frac{p(\hat{x})e^{-\lambda^{-1}d_S(x, \hat{x})}}{\mu(x)} \quad (52)$$

and

$$d_S(x, \hat{x}) = d_{RD}(x, \hat{x}) + \beta d_{IB}(x, \hat{x})$$

Since  $\sum_{\hat{x}} p(\hat{x}|x) = 1$ , substitute it to (52)

$$\mu(x) = \sum_{\hat{x}} p(\hat{x})e^{-\lambda^{-1}d_S(x, \hat{x})} \quad (53)$$

In order to solve such a semantic distortion rate function, it is natural to think of using alternate iteration method to solve it, imitating the traditional rate distortion function. First pick  $\lambda$  and  $\beta$ , and initialize the distribution  $p(\hat{x})$  and  $p(y|\hat{x})$ , **then calculated at the rate constraints to minimize the distortion of  $p(\hat{x}|x)$** . The self consistent equations (43), (44), and (52) are satisfied simultaneously at the minima of the functional  $\mathcal{L}(p(\hat{x}|x))$ . The minimization is done independently over the convex sets of the normalized distributions,  $p(\hat{x})$  and  $p(y|\hat{x})$  and  $p(\hat{x}|x)$ . Namely

$$\min_{p(y|\hat{x})} \min_{p(\hat{x})} \min_{p(\hat{x}|x)} \mathcal{L}(p(\hat{x}|x); p(\hat{x}); p(y|\hat{x})) \quad (54)$$

this minimization is performed by the converging alternating iterations. Denoting by  $k$  the iteration step

$$\begin{cases} p_k(\hat{x}|x) = \frac{p_k(\hat{x})e^{-\lambda^{-1}d_S(x, \hat{x})}}{\sum_{\hat{x}} p_k(\hat{x})e^{-\lambda^{-1}d_S(x, \hat{x})}} \\ p_{k+1}(\hat{x}) = \sum_x p(x)p_k(\hat{x}|x) \\ p_{k+1}(y|\hat{x}) = \sum_y p(y|x)p_k(x|\hat{x}) = \sum_y p(y|x) \frac{p_k(\hat{x}|x)p(x)}{p_k(\hat{x})} \end{cases} \quad (55)$$

when  $p(y|\hat{x})$  is fixed we are back to the rate distortion case with fixed distortion matrix  $d_{RD}(x, \hat{x})$  and  $d_{IB}(x, \hat{x})$ . Then we can use the BA algorithm to solve the optimization problem.

## APPENDIX C

Fig. 9 shows the images reconstructed by the two methods and the corresponding classification results. Intuitively, there are some differences in the images reconstructed by the two








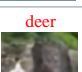
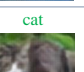


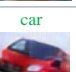

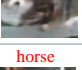
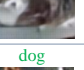

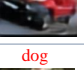
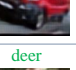






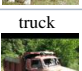

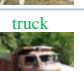


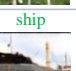






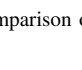
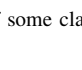
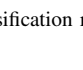
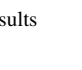


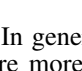
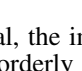
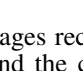
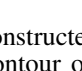
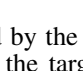
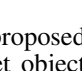
| bpp    | original  | baseline  | proposed  | original  | baseline  | proposed  |
|--------|---|---|---|---|---|---|
| 0.0625 | airplane  | bird  | airplane  | bird  | dog   | bird  |
|        |  |  |  |  |  |  |
|        |  |  |  |  |  |  |
| 0.125  | cat   | deer  | cat   | car   | airplane  | car   |
|        |  |  |  |  |  |  |
|        |  |  |  |  |  |  |
| 0.25   | dog   | horse   | dog   | deer  | dog   | deer  |
|        |  |  |  |  |  |  |
|        |  |  |  |  |  |  |
| 0.5    | truck   | monkey  | truck   | ship  | airplane  | ship  |
|        |  |  |  |  |  |  |
|        |  |  |  |  |  |  |

Fig. 9. Comparison of some classification results

methods. In general, the images reconstructed by the proposed method are more orderly and the contour of the target object is more distinct. These may be the reasons for the improved accuracy of the final classification. Specific feature information is difficult to see directly from the appearance of the picture.

## APPENDIX D

**Fig. 10 shows some comparative images using RFBNet object detection network.** By presenting these result pictures, on the one hand, it is used to show the picture of semantic reconstruction, and on the other hand, it is used to show the specific comparison results of object detection accuracy of baseline and proposed method. In each pair of images, the left side is based on baseline and the right side is based on proposed method.

## APPENDIX E

## REFERENCES

- [1] C. E. Shannon and W. Weaver, *The Mathematical Theory of Communication*. The University of Illinois Press, 1949.
- [2] Emilio Calvanese Strinati, 6G Networks Beyond Shannon Towards Semantic
- [3] Huiqiang Xie, Zhijin Qin, Ye Li. Deep Learning Enabled Semantic Communication Systems. 2020
- [4] Neel Patwa, Nilesh Ahuja, Srinivasa Somayazulu, et.al. Semantic-preserving Image Compression. 2020
- [5] N. Farsad, M. Rao, and A. Goldsmith, Deep learning for joint source-channel coding of text, in *Proc. IEEE Int. Conf. Acoust., Speech Signal Process. (ICASSP)*, Calgary, AB, Canada, Apr. 2018, pp. 2326–2330.
- [6] H. Xie, Z. Qin, G. Ye Li, and B.-H. Juang, “Deep learning enabled semantic communication systems,” 2020, arXiv:2006.10685. [Online]. Available: <http://arxiv.org/abs/2006.10685>
- [7] S. Yao, S. Wang, J. Dai, et al. Semantic-Driven Intelligent Communications for Future Wireless Networks[C]/Poster in 2021 IEEE International Symposium on Information Theory. IEEE, 2021.
- [8] G. K. Wallace, “The JPEG still picture compression standard”, *IEEE Trans. on Consumer Electronics*, vol. 38, no. 1, pp. 43–59, Feb. 1991.
- [9] Majid Rabbani, Rajan Joshi, “An overview of the JPEG2000 still image compression standard”, *ELSEVIER Signal Processing: Image Communication*, vol. 17, no. 1, pp. 3–48, Jan. 2002.
- [10] J. Balle, Valero Laparra, Eero P. Simoncelli, “End-to-End Optimized Image Compression”, *Intl. Conf. on Learning Representations (ICLR)*, pp. 1–27, April 24–26, 2017.
- [11] L. Theis, W. Z. Shi, A. Cunningham and F. Huszar, “Lossy Image Compression with Compressive auto-encoders”, *Intl. Conf. on Learning Representations (ICLR)*, pp. 1–19, April 24–26, 2017.
- [12] G. Toderici, S. M.O’Malley, S. J. Hwang, et al., “Variable rate image compression with recurrent neural networks”, *arXiv: 1511.06085*, 2015.
- [13] Johannes Balle, D. Minnen, S. Singh, S. J. Hwang, N. Johnston, “Variational Image Compression with a Scale Hyperprior”, *Intl. Conf. on Learning Representations (ICLR)*, pp. 1–23, 2018.
- [14] Z. Cheng, H. Sun, M. Takeuchi, et al. Learned Image Compression with Discretized Gaussian Mixture Likelihoods and Attention Modules, *CVPR*, 2020

- [15] N. Tishby, F. C. Pereira, and W. Bialek, The information bottleneck method, in *Proceedings of the 37-th Annual Allerton Conference on Communication, Control and Computing*, 1999, pp. 368–377.
- [16] Naftali Tishby and Noga Zaslavsky, Deep learning and the information bottleneck principle. In *Information Theory Workshop (ITW), 2015 IEEE*, pages 1–5. IEEE, 2015.
- [17] Schwartz-Ziv, Ravid, Tishby, Naftali. Opening the black box of deep neural networks via information. In *arXiv:1703.00810v3 [cs.LG]* 29 Apr 2017.
- [18] Alexander A. Alemi. DEEP VARIATIONAL INFORMATION BOTTLENECK. 2017
- [19] R.Carnap et al., An outline of a theory of semantic information, Res.Lab. Electronics, Massachusetts Inst. Technol., Cambridge MA, RLE Tech. Rep. 247, Oct. 1952.
- [20] J Barwise, J Perry. Situations and attitudes[J]. *The Journal of Philosophy*, 1981,78(11): 668–691.
- [21] L Floridi. Outline of a theory of strongly semantic information[J]. *Minds and machines*, 2004,14(2): 197–221.
- [22] P Zhang, W Xu, et al. Towards Wisdom-Evolutionary and Primitive-Conciseness 6G: A New Paradigm of Semantic Communication Networks[Z]. 2021.
- [23] T. O’Shea and J. Hoydis, An introduction to deep learning for the physical layer, *IEEE Trans. Cogn. Comm. Netw.*, vol. 3, no. 4, pp. 563–575, Dec. 2017.
- [24] C. Lee, J. Lin, P. Chen, et al. Deep Learning-Constructed Joint Transmission-Recognition for Internet of Things. *IEEE Access*, June, 2019
- [25] Y. Yang, et al. Semantic Communications With AI Tasks. 2021
- [26] Mikolaj Jankowski, et al. Deep Joint Source-channel Coding For Wireless Image Retrieval. 2019
- [27] E. Boursoulatz, D. Kurka, D. Gunduz. Deep Joint Source-Channel Coding for Wireless Image Transmission. *IEEE Transactions on Cognitive Communications and Networking*, Vol. 5, No. 3, September 2019
- [28] D. Kurka, D. Gunduz. DeepJSCC-f: Deep Joint Source-Channel Coding of Images with Feedback. *arXiv:1911.11174v2 [cs.IT]* 9 Apr 2020
- [29] Z. Yang, Y. Wang, C. Xu, et al. Discernible Image Compression. *MM ’20*, October 12–16, 2020, Seattle, WA, USA.
- [30] K. Niu, J. Dai, P. Zhang, et al. 6G-oriented Semantic Communications. *Mobile communication*, June, 2021
- [31] Sihui Luo, Yezhou Yang, Mingli Song. DeepSIC: Deep Semantic Image Compression. 2018
- [32] G. J. Sullivan, J. Ohm, W. Han and T. Wiegand, “Overview of the High Efficiency Video Coding (HEVC) Standard”, *IEEE Transactions on Circuits and Systems for Video Technology*, vol. 22, no. 12, pp. 1649–1668, Dec. 2012.
- [33] M. Li, W. Zuo, S. Gu, D. Zhao, D. Zhang, “Learning Convolutional Networks for Contentweighted Image Compression”, *IEEE Conf. on Computer Vision and Pattern Recognition (CVPR)*, June 17–22, 2018.
- [34] C. Cai, L. Chen, X. Zhang, et al. End-to-End Optimized ROI Image Compression, *IEEE Transactions on Image Processing*, vol. 29, 2020
- [35] N. Tishby, N. Slonim, Data clustering by Markovian relaxation and the information bottleneck method, in: *Proceedings of NIPS*, 2000, pp. 640–646.
- [36] N. Friedman, O. Mosenzon, N. Slonim, N. Tishby, Multivariate information bottleneck, in: *Proceedings of UAI*, 2001, pp. 152–161.
- [37] N. Slonim, G. Singh S. Atwal, G. Tkacik, W. Bialek, Information-based clustering, *Proc. Natl. Acad. Sci. USA* (December) (2005).
- [38] Ohad Shamir, Sivan Sabato, Naftali Tishby. Learning and generalization with the information bottleneck. *Theoretical Computer Science*. 2010
- [39] Belghazi, M. I., Baratin, A., Rajeshwar, S., Ozair, S., Bengio, Y., Hjelm, D., and Courville, A. “Mutual information neural estimation”. in *ICML*, 2018.
- [40] P.Y. Cheng, H.W.Tao, S.Y.Dai, et al., “CLUB: A Contrastive Log-ratio Upper Bound of Mutual Information”, in *ICML*, 2020.
- [41] S. Liu, D. Huang, and Y. Wang, “Receptive Field Block Net for Accurate and Fast Object Detection,” *Proceedings of the European Conference on Computer Vision (ECCV)*, pp. 385–400, 2018.
- [42] Yosinski, J., Clune, J., Bengio, Y., Lipson, H.: How transferable are features in deep neural networks? In: *Advances in neural information processing systems*, pp. 3320–3328, 2014.
- [43] Yixin Zhong, A Theory of Semantic Information
- [44] B. R. Bean and E. J. Dutton, *Radio Meteorology*, Dover, 1966.
- [45] *The Radio Refractive Index: Its Formula and Refractivity Data*, ITU-R Rec. P. 453-10, Feb. 2012.
- [46] M. Levy, *Parabolic Equation Methods for Electromagnetic Wave Propagation*, London, U.K.: Inst. Elect. Eng., 2000.
- [47] E. Dinc and O. B. Akan, “Channel model for the surface ducts: large-scale path-loss, delay spread, and AOA,” *IEEE Trans. Antennas Propag.*, vol. 63, no. 6, pp. 2728–2738, Jun. 2015.
- [48] S. F. Mahmoud, H. N. Boghdady and O. L. El-sayed, “Analysis of multipath fading on line-of-sight links in the presence of an elevated atmospheric duct,” *Microwaves, Antennas and Propagation, IEE Proc. H*, vol. 134, no. 1, pp. 71–76, Feb. 1987.
- [49] *Study on Channel Model for Frequencies from 0.5 to 100 GHz*, 3GPP TR 38.901, Sep. 2019.
- [50] C. Szegedy, W. Zaremba, I. Sutskever, J. Bruna, D. Erhan, I. Goodfellow, and R. Fergus. Intriguing properties of neural networks. *arXiv:1312.6199*, 2013.
- [51] C. Guo, F. Liu, S. Chen, C. Feng and Z. Zeng, “Advances on exploiting polarization in wireless communications: Channels, technologies, and applications,” *IEEE Commun. Surveys Tutorials*, vol. 19, no. 1, pp. 125–166, Firstquarter 2017.

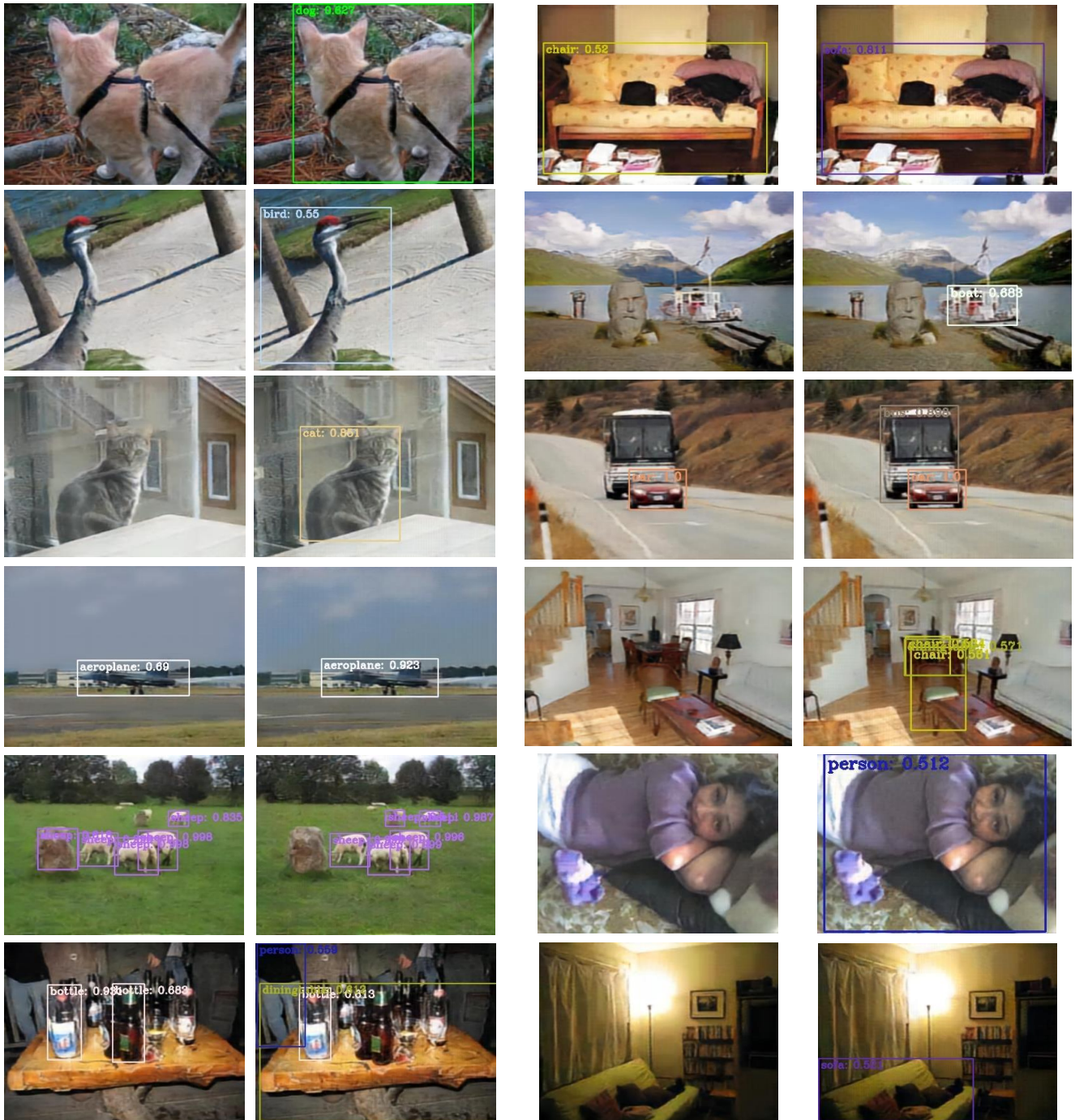


Fig. 10. Comparison of some object detection results, bpp = 0.25.





Fig. 11. object detection different beta show 1, from left to right, from top to bottom,  $\beta$  is equal to 0,  $1e-5$ ,  $1e-4$ ,  $1e-3$ ,  $1e-2$ ,  $1e-1$ , 1, 10,  $\infty$ ,  $\text{bpp} = 0.25$ .

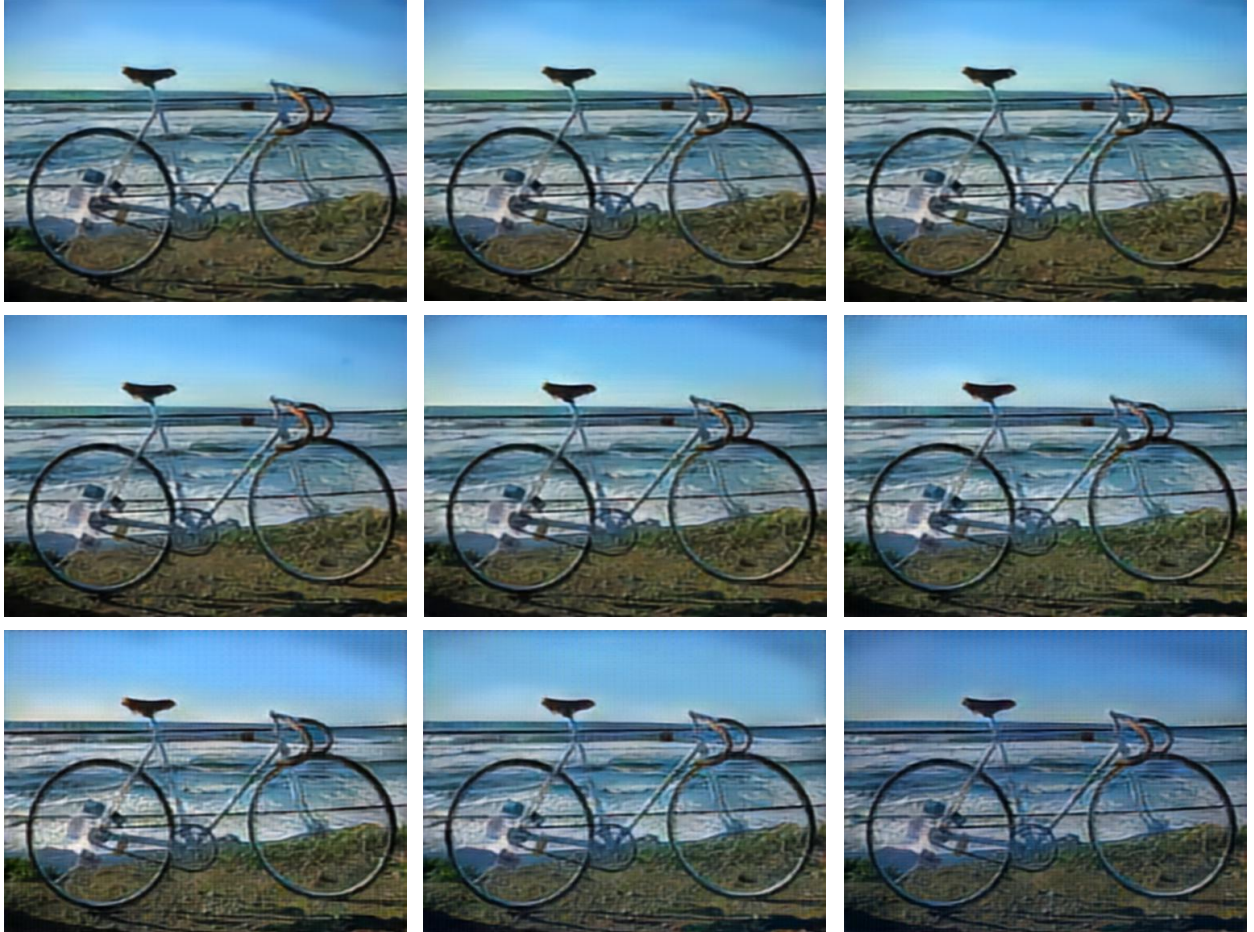


Fig. 12. object detection different beta show 2, from left to right, from top to bottom,  $\beta$  is equal to 0,  $1e-5$ ,  $1e-4$ ,  $1e-3$ ,  $1e-2$ ,  $1e-1$ , 1, 10,  $\infty$ ,  $\text{bpp} = 0.25$ .